Article

Ansa [1]Trochrocenophanes and Their Related Unstrained 1,1‘-Disubstituted Counterparts: Synthesis and Electronic Structure

Holger Braunschweig, Thomas Kupfer, Matthias Lutz, and Krzysztof Radacki

J. Am. Chem. Soc., **2007**, 129 (28), 8893-8906• DOI: 10.1021/ja0724947 • Publication Date (Web): 26 June 2007

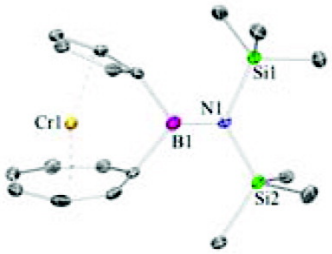

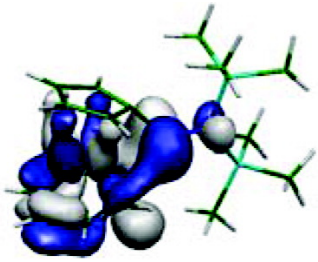

More About This Article

Additional resources and features associated with this article are available within the HTML version:

- Supporting Information
- Links to the 13 articles that cite this article, as of the time of this article download
- Access to high resolution figures
- Links to articles and content related to this article
- Copyright permission to reproduce figures and/or text from this article

View the Full Text HTML

J|A|C|S
ARTICLES
Published on Web 06/26/2007

Ansa [1]Trochrocenophanes and Their Related Unstrained 1,1′-Disubstituted Counterparts: Synthesis and Electronic Structure

Holger Braunschweig,* Thomas Kupfer, Matthias Lutz, and Krzysztof Radacki

Contribution from the Institut für Anorganische Chemie, Julius-Maximilians-Universität Würzburg, Am Hubland, D-97074 Würzburg, Germany

Received April 10, 2007; E-mail: h.braunschweig@mail.uni-wuerzburg.de

Abstract: The heteroleptic sandwich complex [Cr(η^5-C_5H_5)(η^7-C_7H_7)] (trochrocene) was prepared by subsequent treatment of $CrCl_3$ with NaCp and Mg in the presence of cycloheptatriene in yields of 40%. Selective dimetalation employing ^{t}BuLi/tmeda (*N, N, N′, N′*-tetramethylethylenediamine) afforded the highly reactive species [Cr(η^5-C_5H_4Li)(η^7-C_7H_6Li)]·tmeda. An X-ray crystal-structure determination of its thf solvate revealed a symmetrical, dimeric composition in the solid state, that is, a formula of [Cr(η^5-C_5H_4Li)(η^7-C_7H_6-Li)]$_2$·(thf)$_8$, where the C_5H_4 moieties of both units are connected by two bridging lithium atoms. Addition of different element dihalides to the dilithio precursor facilitated the isolation of ansa complexes with boron and germanium in the bridging position. Structural characterization by X-ray diffraction studies on [Cr(η^5-C_5H_4)-BN(SiMe$_3$)$_2$-(η^7-C_7H_6)] and [Cr(η^5-C_5H_4)-GeMe$_2$-(η^7-C_7H_6)] emphasized the strained character with tilt angles of 23.87(13)° and 15.07(17)°, respectively. In contrast, the isolation of the appropriate [1]stannatrochrocenophane failed because of the thermal lability of the resulting product. However, the corresponding 1,1′-disubstitued derivatives [Cr(η^5-C_5H_4R)(η^7-C_7H_6R)] (R = B(Cl)N^{i}Pr$_2$, SiMe$_3$, GeMe$_3$, SnMe$_3$) were obtained by reverse addition of the dilithio precursor to an excess of the element (di)halide. The unstrained nature was proven by a crystal structure analysis of the 1,1′-diborylated species. The electronic structure of these substituted trochrocene derivatives, as well as of the [2]bora and [*n*]sila congeners (n = 1, 2), was investigated by means of UV−vis spectroscopy and DFT methods. As a consequence of the strong electronic influence of the B−N π-system on the LUMOs, the UV−vis studies revealed a complementary correlation of the lowest energy band maxima as a function of molecular distortion for the boron containing species on the one hand, and the boron-free compounds on the other hand. These trends were reproduced fairly well by time dependent DFT calculations.

Introduction

Since the publication of ferrocene, [Fe(η^5-C_5H_5)$_2$], in 1951 by T. J. Kealy and P. L. Pauson[1] and the discovery of bis(benzene)chromium, [Cr(η^6-C_6H_6)$_2$], 4 years later by E. O. Fischer and W. Hafner,[2] the field of organometallic complexes with cyclic π-ligands has been thoroughly investigated. Since then, numerous derivatives were prepared and characterized, including ansa complexes containing bridged carbocycles. These highly strained organometallic molecules have recently been the focus of attention owing to their unique structure, bonding, and reactivity patterns as well as their potential utility as precursors for metal-containing macromolecules.[3] As a consequence of the high stability, the cheap availability, and the well-established dimetalation of ferrocene,[4] [*n*]ferrocenophanes currently rank among the best investigated strained sandwich complexes, and an entire string of different bridging atoms has been realized.[5] Their application in the synthesis of metal containing polymers via ring opening polymerization (ROP) has been described in detail and can be considered as a fundamental highlight in both organometallic chemistry and materials science.[6] It has been shown that the properties of the resulting polymers can easily be controlled depending on the bridging atom, the substituents on the carbocyclic rings, and the

(1) Kealy, T. J.; Pauson, P. L. *Nature* **1951**, *168*, 1039−1040.
(2) (a) Fischer, E. O.; Hafner, Z. Z. *Naturforsch.* **1955**, *10b*, 665−668. (b) Fischer, E. O.; Hafner, Z. Z. *Anorg. Allg. Chem.* **1956**, *286*, 146−148. (c) Seyferth, D. *Organometallics* **2002**, *21*, 1520−1530. (d) Seyferth, D. *Organometallics* **2002**, *21*, 2800−2820.
(3) (a) Foucher, D. A.; Honeyman, C. H.; Nelson, J. M.; Tang, B. Z.; Manners, I. *Angew. Chem.* **1993**, *105*, 1843−1845; *Angew. Chem., Int. Ed.* **1993**, *32*, 1709−1711. (b) Manners, I. *Adv. Organomet. Chem.* **1995**, *37*, 131−168. (c) Herberhold, M. *Angew. Chem.* **1995**, *107*, 1985−1987; *Angew. Chem., Int. Ed.* **1995**, *34*, 1837−1839. (d) Braunschweig, H.; Dirk, R.; Englert, U.; Berenbaum, A.; Green, J. C.; Lough, A. J.; Manners, I. *J. Am. Chem. Soc.* **2000**, *122*, 5765−5774. (e) Mizuta, T.; Imamura, Y.; Miyoshi, K. *J. Am. Chem. Soc.* **2003**, *125*, 2068−2069. (f) Braunschweig, H.; Breitling, F. M.; Gullo, E.; Kraft, M. *J. Organomet. Chem.* **2003**, *680*, 31−42. (g) Aldridge, S.; Bresner, C. *Coord. Chem. Rev.* **2003**, *244*, 71−92. (h) Braunschweig, H.; Lutz, M.; Radacki, K. *Angew. Chem.* **2005**, *117*, 5792−5796, *Angew. Chem., Int. Ed.* **2005**, *44*, 5647−5651.
(4) Rausch, M.; Ciappenelli, D. *J. Organomet. Chem.* **1967**, *13*, 127−136.
(5) (a) Osborne, A. G.; Whiteley, R. H. *J. Organomet. Chem.* **1975**, *101*, C27−C28. (b) Seyferth, D.; Whiters, H. P. *Organometallics* **1982**, *1*, 1275−1282. (c) Broussier, R.; Da, Rold, A.; Gautheron, B.; Dromzee, Y.; Leannin, Y. *Inorg. Chem.* **1990**, *29*, 1817−1822. (d) Buretea, M. A.; Tilley, T. D. *Organometallics* **1997**, *16*, 1507−1510. (e) Rulkens, R.; Gates, D. P.; Balaishis, D.; Pudelski, J. K.; McIntosh, D. F.; Lough, A. J.; Manners, I. *J. Am. Chem. Soc.* **1997**, *119*, 10976−10986. (f) Jäkle, F.; Rulkens, R.; Zech, G.; Foucher, D. A.; Lough, A. J.; Manners, I. *Chem.−Eur. J.* **1998**, *4*, 2117−2128. (g) Schachner, J. A.; Lund, C. L.; Quail, J. W.; Müller, J. *Organometallics* **2005**, *24*, 785−787. (h) Schachner, J. A.; Lund, C. L.; Quail, J. W.; Müller, J. *Organometallics* **2005**, *24*, 4483−4488.

bridging element(s), respectively, as well as on the polymerization technique employed during their synthesis. The intrinsic molecular ring strain is also reflected by an enhanced reactivity of the strained bond between the cyclopentadienyl ligand and the bridging element(s),[5f,7] between the bridging elements,[3h,8] or the Fe−Cp bond,[3d,e,9] which led to the isolation of several insertion and ring opening products. As a striking example, the transition metal mediated diboration of alkynes by strained [2]metallocenophanes may be mentioned in this context, which could be achieved for the first time under heterogeneous conditions.[8b] In contrast to this mature field, examples of ansa metallocenes containing other metal centers than iron are rare and comprise only few derivatives of chromium,[10] ruthenium,[11] cobalt,[12] and nickel.[13] Similarily, the chemistry of the related bis(benzene)metal complexes has been scarcely studied in comparison to the ferrocene system, hence, the number of ansa complexes is truncated to a few examples of bridged bis(benzene)vanadium, [V(η^6-C_6H_6)$_2$],[14] and bis(benzene)chromium derivatives.[8b,14,15]

In addition, heteroleptic sandwich compounds, for instance those capped by cyclopentadienyl (Cp) and cycloheptatrienyl (Cht) rings, have only been utilized very recently in the synthesis of silicon- and boron-bridged derivatives of titanium and vanadium, respectively. These complexes were obtained by metalation of the parent sandwich complexes [Ti(η^5-C_5H_5)(η^7-C_7H_7)] (troticene)[16] and [V(η^5-C_5H_5)(η^7-C_7H_7)] (trovacene)[17] applying BuLi in the presence of *N*, *N*, *N*′, *N*′-tetramethylethylendiamine (tmeda) followed by treatment of the intermediate dilithio complex with the appropriate element dihalides. Polymerization experiments confirmed their susceptibility to strain release by undergoing transition metal mediated ROP to yield oligomeric materials.[16] However, the highly reactive dilithiated sandwich precursors are usually not isolated nor characterized, e.g., by X-ray diffraction, even though their structural parameters are of great interest. In fact, structural data of metalated sandwich complexes are actually rare to date, though several examples are reported in the literature, for instance the long known dilithiated ferrocene derivatives [Fe(η^5-C_5H_4Li)$_2$]·pmdta[18] (pmdta = *N*, *N*′, *N*′, *N*″, *N*″-pentamethyldiethylentriamine) and [Fe(η^5-C_5H_4Li)$_2$]$_3$·(tmeda)$_2$.[19] Recently, Mulvey and co-workers accomplished the selective tetrametalation of ferrocene and its higher homologues,[20] the synergic monodeprotonation of bis(benzene)chromium,[21] and the selective dimetalation of ferrocene[22] by mixed alkali metal−magnesium amide bases along with the appropriate crystal structure analyses. Selective dimetalation of ferrocene was also achieved by alkali-metal-mediated manganation, in which case manganese was for the first time directly attached to an aromatic framework.[23a] A related ferrocene derivative was prepared by Wagner et al. by the transmetalation reaction of dilithiated ferrocene with $FeCl_2$ that yielded an pentanuclear Fe^{II} cluster with two bridging iron centers.[23b] The crystal structures of selectively mono- and dimetalated ferrocenylcopper,[24] dilithiated [Mn(η^5-C_5H_5)(η^6-C_6H_6)],[25] as well as dilithiated bis(benzene)molybdenum, [Mo(η^6-C_6H_6)$_2$],[26] further contributed to the understanding of the fundamentals that determine the conformation of this class of organometallic compounds.

In the course of our recent studies on strained metalloarenophanes, we became interested in [Cr(η^5-C_5H_5)(η^7-C_7H_7)] (trochrocene), whose derivatization to form the [2]bora (**1**),[3h]

(6) (a) Foucher, D. A.; Tang, B.-Z.; Manners, I. *J. Am. Chem. Soc.* **1992**, *114*, 6246−6248. (b) Nguyen, P.; Gómez-Elipe, P.; Manners, I. *Chem. Rev.* **1999**, *99*, 1515−1548. (c) Manners, I. *Chem. Commun.* **1999**, 857−865. (d) MacLachlan, M. J.; Ginzburg, M.; Coombs, N.; Coyle, T. W.; Raju, N. P.; Greedan, J. E.; Ozin, G. A.; Manners, I. *Science* **2000**, *287*, 1460−1463. (e) Manners, I. *Science* **2001**, *294*, 1664−1666. (f) Arsenault, A. C.; Míguez, H.; Kitaev, V.; Ozin, G. A.; Manners, I. *Adv. Mater* **2003**, *15*, 503−507. (g) Clendenning, S. B.; Han, S.; Coombs, N.; Paquet, C.; Rayat, M. S.; Grozea, D.; Brodersen, P. M.; Sodhi, R. N. S.; Yip, C. M.; Lu, Z.-H.; Manners, I. *Adv. Mater* **2004**, *16*, 291−296.

(7) (a) Sheridan, J. B.; Lough, A. J.; Manners, I. *Organometallics* **1996**, *15*, 2195−2197. (b) Sheridan, J. B.; Temple, K.; Lough, A. J.; Manners, I. *J. Chem. Soc., Dalton Trans.* **1997**, 711−713. (c) Mizuta, T.; Onishi, M.; Miyoshi, K. *Organometallics* **2000**, *19*, 5005−5009. (d) Mizuta, T.; Onishi, M.; Nakazono, T.; Nakazawa, H.; Miyoshi, K. *Organometallics* **2002**, *21*, 717−726.

(8) (a) Finckh, W.; Tang, B.-Z.; Lough, A. J.; Manners, I. *Organometallics* **1992**, *11*, 2904−2911. (b) Braunschweig, H.; Kupfer, T.; Lutz, M.; Radacki, K.; Seeler, F.; Sigritz, R. *Angew. Chem.* **2006**, *118*, 8217−8220; *Angew. Chem., Int. Ed.* **2006**, *45*, 8048−8051.

(9) Tanabe, M.; Bourke, S. C.; Herbert, D. E.; Lough, A. J.; Manners, I. *Angew. Chem.* **2005**, *117*, 6036−6040; *Angew. Chem., Int. Ed.* **2005**, *44*, 5886−5890.

(10) (a) Matare, G. J.; Foo, D. M.; Kane, K. M.; Zehnder, R.; Wagener, M.; Shapiro, P. J.; Concolino, T.; Rheingold, A. L. *Organometallics* **2000**, *19*, 1534−1539. (b) Sinnema, P.-J.; Nairn, J.; Zehnder, R.; Shapiro, P. J.; Twamley, B.; Blumenfeld, A. *Chem. Commun.* **2004**, 110−111. (c) Schaper, F.; Wrobel, O.; Schwörer, R.; Brintzinger, H.-H. *Organometallics* **2004**, *23*, 3552−3555. (d) Shapiro, P. J.; Zehnder, R.; Foo, D. M.; Perrotin, P.; Budzelaar, P. H. M.; Leitch, S.; Twamley, B. *Organometallics* **2006**, *25*, 719−732.

(11) (a) Nelson, J. M.; Lough, A. J.; Manners, I. *Angew. Chem.* **1994**, *106*, 1019−1021, *Angew. Chem., Int. Ed.* **1994**, *33*, 989−991. (b) Nelson, M.; Lough, A. J.; Manners, I. *Organometallics* **1994**, *13*, 3703−3710. (c) Vogel, U.; Lough, A. J.; Manners, I. *Angew. Chem.* **2004**, *116*, 3383−3387; *Angew. Chem., Int. Ed.* **2004**, *33*, 989−991.

(12) (a) Drewitt, M. J.; Barlow, S.; O'Hare, D.; Nelson, J. M.; Nguyen, P.; Manners, I. *Chem. Commun.* **1996**, 2153−2154. (b) Fox, S.; Dunne, J.; Tacke, M.; Schmitz, D.; Dronskowski, R. *Eur. J. Inorg. Chem.* **2002**, 3039−3046.

(13) Buchowicz, W.; Jerzykiewicz, L. B.; Krasinska, A.; Losi, S.; Pietrzykowski, A.; Zanello, P. *Organometallics* **2006**, *25*, 5076−5082.

(14) (a) Elschenbroich, C.; Hurley, J.; Metz, B.; Massa, W.; Baum, G. *Organometallics* **1990**, *9*, 889−897. (b) Elschenbroich, C.; Bretschneider-Hurley, A.; Hurley, J.; Massa, W.; Wocadlo, S.; Pebler, J. *Inorg. Chem.* **1993**, *32*, 5421−5424. (c) Elschenbroich, C.; Bretschneider-Hurley, A.; Hurley, J.; Behrendt, A.; Massa, W.; Wocadlo, S.; Reijerse, E. *Inorg. Chem.* **1995**, *34*, 743−745. (d) Elschenbroich, C.; Schmidt, E.; Gondrum, R.; Metz, B.; Burghaus, O.; Massa, W.; Wocadlo, S. *Organometallics* **1997**, *16*, 4589−4596. (e) Lund, C. L.; Schachner, J. A.; Quail, J. W.; Müller, J. *Organometallics* **2006**, *25*, 5817−5823.

(15) (a) Hultzsch, K. C.; Nelson, J. M.; Lough, A. J.; Manners, I. *Organometallics* **1995**, *14*, 5496−5502. (b) Braunschweig, H.; Homberger, M.; Hu, C.; Zheng, X.; Gullo, E.; Clentsmith, G. K. B.; Lutz, M. *Organometallics* **2004**, *23*, 1968−1970.

(16) (a) Tamm, M.; Kunst, A.; Bannenberg, T.; Herdtweck, E.; Sirsch, P.; Elsevier, C. J.; Ernsting, J. M. *Angew. Chem.* **2004**, *116*, 5646−5650; *Angew. Chem., Int. Ed.* **2004**, *43*, 5530−5534. (b) Tamm, M.; Kunst, A.; Herdtweck, E. *Chem. Commun.* **2005**, 1729−1731. (c) Tamm, M.; Kunst, A.; Bannenberg, T.; Randoll, S.; Jones, P. G. *Organometallics* **2007**, *26*, 417−424.

(17) (a) Elschenbroich, C.; Paganelli, F.; Nowotny, M.; Neumüller, B.; Burghaus, O. *Z. Anorg. Allg. Chem.* **2004**, *630*, 1599−1606. (b) Braunschweig, H.; Lutz, M.; Radacki, K.; Schaumlöffel, A.; Seeler, F.; Unkelbach, C. *Organometallics* **2006**, *25*, 4433−4435.

(18) Walczak, M.; Walczak, K.; Mink, R.; Rausch, M. D.; Stucky, G. *J. Am. Chem. Soc.* **1978**, *100*, 6382−6388.

(19) Butler, I. R.; Cullen, W. R.; Ni, J.; Rettig, S. J. *Organometallics* **1985**, *4*, 2196−2201.

(20) (a) Clegg, W.; Henderson, K. W.; Kennedy, A. R.; Mulvey, R. E.; O'Hara, C. T.; Rowlings, R. B.; Tooke, D. M. *Angew. Chem.* **2001**, *113*, 4020−4023; *Angew. Chem., Int. Ed.* **2001**, *40*, 3902−3906. (b) Andrikopoulos, P. C.; Armstrong, D. R.; Clegg, W.; Gilfillan, C. J.; Hevia, E.; Kennedy, A. R.; Mulvey, R. E.; O'Hara, C. T.; Parkinson, J. A. *J. Am. Chem. Soc.* **2004**, *126*, 11612−11620.

(21) Hevia, E.; Honeyman, G. W.; Kennedy, A. R.; Mulvey, R. E.; Sherrington, D. C. *Angew. Chem.* **2005**, *117*, 70−74; *Angew. Chem., Int. Ed.* **2005**, *44*, 68−72.

(22) Henderson, K. W.; Kennedy, A. R.; Mulvey, R. E.; O'Hara, C. T.; Rowlings, R. B. *Chem, Commun.* **2001**, 1678−1679.

(23) (a) Garcia-Álvarez, J.; Kennedy, A. K.; Klett, J.; Mulvey, R. E. *Angew. Chem.* **2007**, *119*, 1123−1126; *Angew. Chem., Int. Ed.* **2007**, *46*, 1105−1108. (b) Sänger, I.; Heilmann, J. B.; Bolte, M.; Lerner, H.-W.; Wagner, M. *Chem. Commun.* **2006**, 2027−2029.

(24) Venkatasubbaiah, K.; DiPasquale, A. G.; Bolte, M.; Rheingold, A. L.; Jäkle, F. *Angew. Chem.* **2006**, *118*, 6992−6995; *Angew. Chem., Int. Ed.* **2006**, *45*, 6838−6841.

(25) Braunschweig, H.; Kupfer, T.; Radacki, K. *Angew. Chem.* **2007**, *119*, 1655−1558; *Angew. Chem., Int. Ed.* **2007**, *46*, 1630−1633.

(26) Braunschweig, H.; Buggisch, N.; Englert, U.; Homberger, M.; Kupfer, T.; Leusser, D.; Lutz, M.; Radacki, K. *J. Am. Chem. Soc.* **2007**, *125*, 4840−4846.

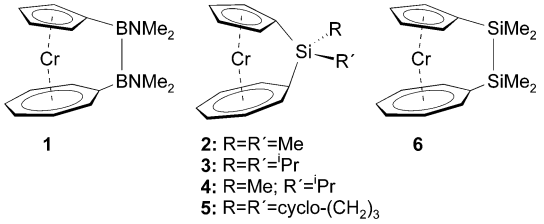

1 **2:** R=R´=Me **6**
3: R=R´=^{i}Pr
4: R=Me; R´=^{i}Pr
5: R=R´=cyclo-$(CH_2)_3$

the [1]sila (**2**−**5**) and the [2]sila (**6**) derivatives we have reported.[27] The reactive dilithiated precursor has been prepared by treatment of the parent sandwich complex with ^{t}BuLi/tmeda in alipahtic solvents and has been isolated, as well as fully characterized by NMR spectroscopy. The ansa-bridged species exhibit weak to moderate molecular strain, as indicated by the corresponding tilt angles α, ranging from 2.60° for **6** to 16.33° for the silicon-bridged derivative **5**. However, the ring strain present in **1** and **2** was proven by a facile oxidative addition reaction with $[Pt(PEt_3)_3]$ that led to the insertion of the low-valent transition metal into the bridging B−B bond and the *ipso*-C_{Cht}−silicon bond, respectively. Additionally, [1]silatrochrocenophane **2** was successfully polymerized in the presence of Karstedt's catalyst to yield materials with moderate molecular weights ($M_W = 6.4 \times 10^3$).

The molecular ring strain, and hence the polymerization behavior, can easily be tuned by the systematic variation of the bridging elements. In this contribution, we report full details of our work on the synthesis and structural characterization of the first [1]bora-, [1]germa- and [1]stannatrochrocenophanes, as well as on the preparation of the corresponding unstrained 1,1′-disubstituted derivatives. We also discuss the electronic structures of these molecules, which were investigated by means of UV−vis spectroscopy and theoretical calculations.

Results and Discussion

Synthesis of [Cr(η^5-C_5H_5)(η^7-C_7H_7)]. The synthesis of trochrocene was originally reported by E. O. Fischer and S. Breitschaft in the 1960s by a multistep reaction sequence (Scheme 1) with an overall yield of 14%, at best.[28] However, in our hands the yields were not reproducible at all, fluctuating in a range of 0−10%. As a consequence, these preparative drawbacks prompted us to reinvestigate the described procedure and to further develop a more convenient protocol. As depicted in Scheme 1, the yield determining step during the synthesis of trochrocene comprises the formation of [Cr(η^5-C_5H_5)(η^6-C_6H_6)],[28b] which is obtained in 22% yield at most. Hence, we treated the crude product directly with cyclohepatriene in the presence of $AlCl_3$, and after workup we were able to isolate trochrocene in essentially identical yields; that is, the isolation of the intermediate is not a necessary prerequisite for this reaction. However, the sublimation of crude trochrocene was always accompanied by the appearance of a green rim right above the heating source that could be separated mechanically from the desired product. After a time-consuming purification procedure (column chromatography and repeated recrystallization steps) this compound was identified by NMR spectroscopy as the cyclopentadienyl ring-phenylated derivative **7**.

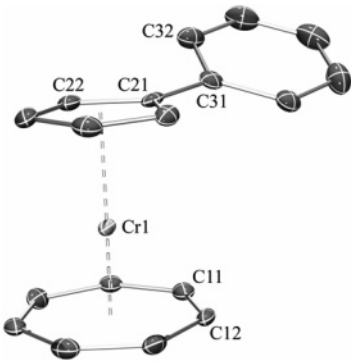

Figure 1. Molecular structure of **7**. Only one molecule of the asymmetric unit is shown for clarity. Selected bond lengths [Å] and angles [deg]: Cr1−C11, 2.164(3); Cr1−C12, 2.156(3); Cr1−C13, 2.169(3); Cr1−C14, 2.170(4); Cr1−C15, 2.171(4); Cr1−C16, 2.175(4); Cr1−C17, 2.168(3); Cr1−C21, 2.196(4); Cr1−C22, 2.183(4); Cr1−C23, 2.193(4); Cr1−C24, 2.178(4); Cr1−C25, 2.171(4); C21−C31, 1.477(5); Cr1−X_{Cp}, 1.819; Cr1−X_{Cht}, 1.439; C22−C21−C31−C32, 22.34(57); X_{Cp}−Cr1−X_{Cht}, 178.1 (X_{Cp}, X_{Cht} = centroids of the C_5H_4 and the C_7H_7 rings, respectively).

Scheme 1. Original Procedure for the Preparation of Trochrocene

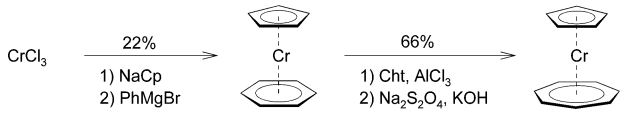

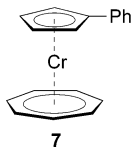

7

Thus, the resonance signals of the ring protons in the ^{1}H NMR spectrum display a splitting pattern, which is in agreement with a trochrocene derivative substituted exclusively at the C_5H_4 moiety. Hence, the α and β hydrogen atoms of the Cp ring show two distinct multiplets (δ = 3.75 and 4.17), whereas the Cht hydrogen atoms exhibit a slightly broadend singlet at δ = 5.33 with an integration ratio of 2:2:7. As expected for an unstrained sandwich complex, these signals appear in the same region as those found in the parent trochrocene complex (δ = 3.66 and 5.45 ppm).

The proposed constitution was authenticated in the solid-state structure of **7** (Figure 1). **7** crystallizes in the monoclinic space group $P2_1$ with two independent molecules in the asymmetric unit, whereas the structural parameters of both moieties differ only marginally. Hence, for simplicity reasons only one of the molecular structures is discussed below. Bond distances and bond angles within the sandwich motif are unremarkable. The Cr−C bond distances [C_5H_4, 2.171(4)−2.196(4) Å; C_7H_7, 2.156(3)−2.175(4) Å] strongly resemble the values found in the unsubstituted sandwich precursor [2.147−2.167(4) Å].[29] The unstrained character of **7** is reflected by the following: (1) the two aromatic ring moieties are planar, therefore a regular η^5- and η^7-coordination can be assumed; (2) both rings are arranged almost parallel with an angle between the planes of the C_5H_4 and the C_7H_7 moieties of 1.42(22)°; (3) the angle δ, defined by

(27) Bartole−Scott, A.; Braunschweig, H.; Kupfer, T.; Lutz, M.; Manners, I.; Nguyen, T.-I.; Radacki, K.; Seeler, F. *Chem.—Eur. J.* **2006**, *12*, 1266−1273.

(28) (a) Fischer, E. O.; Breitschaft, S. *Angew. Chem.* **1963**, *75*, 94−95; *Angew. Chem., Int. Ed.* **1963**, *2*, 44. (b) Fischer, E. O.; Breitschaft, S. *Chem. Ber.* **1966**, *99*, 2213−2226. (c) Fischer, E. O.; Breitschaft, S. *Chem. Ber.* **1966**, *99*, 2905−2916.

(29) Lyssenko, K. A.; Antipin, M. Yu.; Ketkov, S. Yu. *Russ. Chem. Bull., Int. Ed.* **2001**, *50*, 130−141.

Scheme 2. Improved Synthesis of $[Cr(\eta^5\text{-}C_5H_5)(\eta^7\text{-}C_7H_7)]$

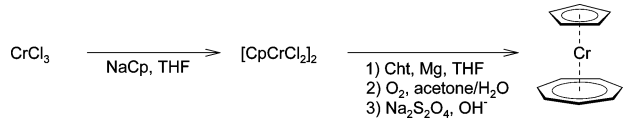

the ring centroids and the metal center, exhibits only a minimal deviation from the ideal linear alignment found in the parent compound (δ = 178.1°). For sterical reasons, the phenyl substitutent attached to the Cp ring is notedly distorted from a coplanar arrangement [C22−C21−C31−C32 = 22.34(57)°].

The formation of **7** as a side product must have occurred during the first step of the trochrocene synthesis, that is, the preparation of $[Cr(\eta^5\text{-}C_5H_5)(\eta^6\text{-}C_6H_6)]$ (Scheme 1),[28b] and might be explained by deprotonation of the five-membered ring and subsequent reductive coupling with one molecule PhMgBr to yield $[Cr(\eta^5\text{-}C_5H_4Ph)(\eta^6\text{-}C_6H_6)]$, which is then converted to the trochrocene derivative **7**. In addition, the generation of other ring-phenylated mono- and dinuclear species derived from the biphenyl moiety, such as $[(\eta^5\text{-}C_5H_5)Cr(\mu_2,\eta^6,\eta^6\text{-}C_{12}H_{10})Cr(\eta^5\text{-}C_5H_5)]$ and $[Cr(\eta^5\text{-}C_5H_5)(\eta^6\text{-}C_6H_5Ph)]$, must be taken into account as possible byproducts. Related biphenyl complexes have been observed and isolated during the synthesis of the corresponding manganese compound, $[Mn(\eta^5\text{-}C_5H_5)(\eta^6\text{-}C_6H_6)]$, in which case they even represent the main products.[28b] Thus, the reason for the low yield synthesis of $[Cr(\eta^5\text{-}C_5H_5)(\eta^6\text{-}C_6H_6)]$, and consequently that of trochrocene, is given by the low selectivity of the reaction and the formation of several side products. Within the second step of the preparation of trochrocene, the $AlCl_3$-mediated ring exchange, the biphenyl containing species are transmuted to trochrocene and, hence, cannot be observed after workup.

To avoid the formation of the ring-phenylated side products emerging during the original Fischer protocol and to further develop a more convenient synthetic access to trochrocene, we followed a different known reaction sequence that was already successfully employed in the preparation of the analogous titanium and zirconium sandwich species, $[M(\eta^5\text{-}C_5H_5)(\eta^7\text{-}C_7H_7)]$ (M = Ti,[30] Zr[31]). Accordingly, trochrocene has been obtained in yields up to 40% by treatment of $[(\eta^5\text{-}C_5H_5)CrCl_2]_2$, prepared in situ from equimolar amounts $CrCl_3$ and NaCp, with magnesium turnings in the presence of excess cycloheptatriene in THF (Scheme 2). In contrast to the syntheses of the Ti and Zr analogues, the presence of catalytic amounts of $FeCl_3$ had no impact on this particular reaction.

In our hands, the isolation of trochrocene directly from the crude reaction mixture via sublimation turned out to be quite difficult owing to polymeric organic side products arising from the cycloheptatriene. In addition, the yields obtained were not satisfactory at all (5−10%). We found it more valuable to follow an oxidation−reduction cycle at this point (Scheme 2). Thus, the crude trochrocene was oxidized to the corresponding cation by refluxing the reaction mixture in acetone/H_2O under air exposure. The resulting water soluble green cation was subsequently reduced with $Na_2S_2O_4$ in toluene/water under an inert atmosphere to yield a dark blue solution of pure trochrocene. Additional purification of the air-sensitive product was achieved by means of sublimation at 100 °C and 10^{-3} mbar, yielding dark-blue crystals of $[Cr(\eta^5\text{-}C_5H_5)(\eta^7\text{-}C_7H_7)]$. Given the availability of gram quantities of trochrocene, our intention was to further investigate the chemistry of this sandwich complex and of strained [*n*]trochrocenophanes in particular.

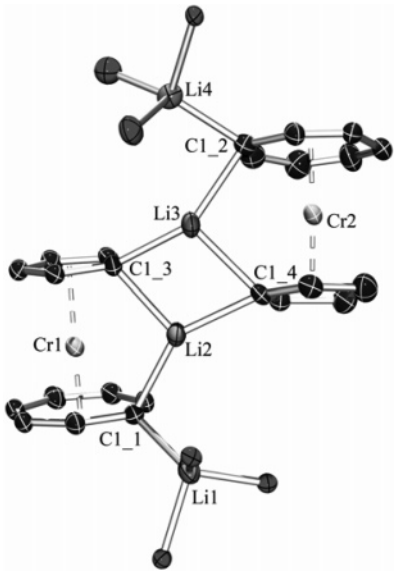

Figure 2. Molecular structure of the $[Cr(\eta^5\text{-}C_5H_4Li)(\eta^7\text{-}C_7H_6Li)]_2\cdot(thf)_8$ (**8**) solvate. For clarity, only the oxygen atoms of the thf molecules are shown and thf molecules incorporated in the crystal lattice are omitted. Selected bond lengths [Å] and angles [deg]: Li1−Li2, 3.024(7); Li2−Li3, 2.416(6); Li3−Li4, 2.848(6); Li1−C1_1, 2.123(6); Li2−C1_1, 2.107(5); Li2−C1_3, 2.179(5); Li2−C1_4, 2.138(5); Li3−C1_2, 2.182(5); Li3−C1_3, 2.135(5); Li3−C1_4, 2.207(5); Li4−C1_2, 2.134(5); Cr1−C_{Cp}, 2.159(3)−2.272(2) [av. 2.084(3)]; Cr1−C_{Cht}, 2.109(2)−2.254(2) [av. 2.158(3)]; Cr2−C_{Cp}, 2.109(3)−2.242(2) [av. 2.191(3)]; Cr2−C_{Cht}, 2.088(4)−2.233(2) [av. 2.162(3)]; Cr1−X_{Cp}, 1.838; Cr1−X_{Cht}, 1.419; Cr2−X_{Cp}, 1.777; Cr2−X_{Cht}, 1.482; C1_1−Li2−C1_3, 101.75(18); C1_1−Li2−C1_4, 142.83(21); C1_3−Li2−C1_4, 110.86(21); C1_2−Li3−C1_3, 141.72(25); C1_2−Li3−C1_4, 97.61(17); C1_3−Li3−C1_4, 109.94(21); X_{Cp}−Cr1−X_{Cht}, 178.0; X_{Cp}−Cr2−X_{Cht}, 176.3 (X_{Cp}, X_{Cht} = centroids of the C_5H_4 and the C_7H_6 rings, respectively).

Dimetalation. We recently reported on the facile dilithiation of trochrocene to afford the highly reactive species $[Cr(\eta^5\text{-}C_5H_4Li)(\eta^7\text{-}C_7H_6Li)]\cdot$tmeda (**8**·tmeda), which was fully characterized by NMR spectroscopic experiments.[3h] The selectivity of the dimetalation was confirmed by the ^1H NMR data, which showed the presence of a single compound with the expected splitting pattern and integration ratio. The conformation of this species was unambiguously demonstrated by the determination of the solid-state structure. Thus, recrystallization of **8**·tmeda from a saturated thf solution at −70 °C yielded pale brown crystals that were formulated as **8**·$(thf)_3$ on the basis of ^1H NMR spectroscopy; that is, dissolving in thf causes the replacement of the tmeda ligand by coordinating thf molecules. As expected, the NMR spectroscopic data in $[D_8]$-thf solution are very similiar to those of the tmeda adduct (**8**·tmeda).[3h] The crystals obtained were of sufficient quality; hence, the molecular structure of the dilithiated precursor (**8**) was determined by crystal structure analysis (Figure 2). In the solid state, **8** exhibits a symmetrical dimeric structure, in which both molecules are connected by two bridging lithium atoms (Li2 and Li3) bound to the ipso carbons of both C_5H_4 moieties, as well as to one ipso carbon of the C_7H_6 rings. In contrast, the terminal lithium atoms (Li1 and Li4) are bound to the ipso carbon of the seven-membered rings and are both further stabilized by the coordination of three thf

(30) Demerseman, B.; Dixneuf, P. H.; Douglade, J.; Mercier, R. *Inorg. Chem.* **1982**, *21*, 3942−3947.
(31) Tamm, M.; Kunst, A.; Bannenberg, T.; Herdtweck, E.; Schmid, R. *Organometallics* **2005**, *24*, 3163−3171.

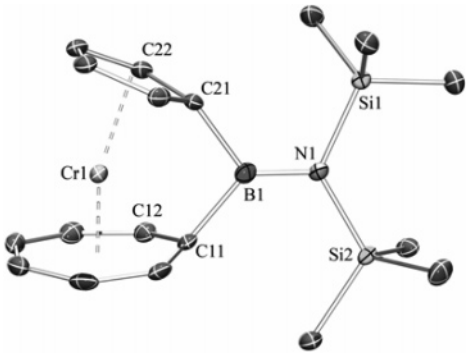

Figure 3. Molecular structure of **9**. Selected bond lengths [Å] and angles [deg]: Cr1−C11, 2.069(3); Cr1−C12, 2.132(3); Cr1−C13, 2.182(3); Cr1−C14, 2.176(3); Cr1−C15, 2.180(3); Cr1−C16, 2.181(3); Cr1−C17, 2.140(3); Cr1−C21, 2.126(3); Cr1−C22, 2.156(3); Cr1−C23, 2.213(3); Cr1−C24, 2.219(3); Cr1−C25, 2.161(3); C11−B1, 1.620(4); C21−B1, 1.629(4); B1−N1, 1.399(4); Cr1−X_{Cp}, 1.808; Cr1−X_{Cht}, 1.409; C11−B1−C21, 100.52(52); C11−B1−N1, 130.98(25); C21−B1−N1, 128.47(26); X_{Cp}−Cr1−X_{Cht}, 162.0 (X_{Cp}, X_{Cht} = centroids of the C_5H_4 and the C_7H_6 rings, respectively).

oxygen atoms. The presence of the thf molecules results in two severe consequences: (1) even though the crystals showed an absolutely proper morphology under the microscope, they did not scatter any further than to a resolution of ∼1 Å; (2) the thf molecules show extensive disorder, thus requiring a combination of constraints and restraints in the refinement, and as a consequence, the structural parameters within these moieties are excluded from the following discussion. In agreement with the molecular structures of [Cr(η^5-C_5H_5)(η^7-C_7H_7)][29] and **7**, the chromium CH carbon bond distances to the five-membered rings [2.109(3)−2.184(2) Å] are comparable to those to the seven-membered rings [2.088(4)−2.173(2) Å]. However, the chromium ipso carbon bonds are significantly elongated both for the C_5H_4 [2.242(2) and 2.172(2) Å] and the C_7H_6 moieties [2.233(2) and 2.254(2) Å]. As expected, the two aromatic ring substitutents of each chromium unit are arranged almost parallel to each other; angles between the planes of the five- and seven-membered rings amount to 1.23° and 1.61°, respectively. The unstrained character of this structural motif is also demonstrated by the angles δ (vide supra), which reflect almost linear arrangements in both subunits [Cr1, 178.0° and Cr2, 176.3°]. The tetra-coordinated terminal lithium atoms Li1 and Li4 display a tetrahedral environment, whereas the coordination sphere of the unsaturated bridging lithium atoms Li2 and Li3 is best described as a distorted trigonal planar geometry [ΣLi2 = 355.4° and ΣLi3 = 349.3°]. Both the Li−C bond distances[18,19] [2.107(5)−2.207(5) Å] and the Li−O bond lengths[32] [1.856(4)−2.017(6) Å] lie within previously reported ranges. The Li···Li separation distance between the bridging lithium atoms [Li2···Li3 = 2.416(6) Å] differs significantly from those to the terminal lithium atoms [Li1···Li2 = 3.024(7) Å and Li3···Li4 = 2.848(6) Å], which is in agreement with the structural parameters found in the related dilithiated manganese complex [Mn(η^5-C_5H_4Li)(η^6-C_6H_5Li)]·pmdta.[25] The relative short value of the former is comparable to that found in cylohexyllithium [2.397 Å][33] and might suggest a direct lithium−lithium interaction, in terms of stabilizing the unsaturated lithium centers. However, according to earlier investigations on alkyllithium reagents[34] or the related dilithiated ferrocene derivative [Fe(η^5-$C_5H_4Li)_2$]·pmdta,[18] this type of stabilization is weak at best.

[1]Trochrocenophanes. In our recent publications we successfully demonstrated the conversion of **8**·tmeda to several strained [1]trochrocenophanes containing silicon in the bridging position.[27] Hence, current work has focused on the incorporation of other main-group elements into the ansa bridge. Accordingly, the highly strained [1]boratrochrocenophanes **9** and **10**, as well as the germanium bridged derivative **11** were prepared by stoichiometric treatment of **8**·tmeda at −78 °C with the appropriate element dihalides in aliphatic or aromatic solvents, respectively. These compounds were isolated after workup as highly colored, crystalline materials in good yields of 60−70% (Scheme 3).

The introduction of the small boron bridge into **9** and **10** results in a splitting of the corresponding resonance signals of the aromatic ring protons in the ^{1}H NMR spectra in comparison to the parent sandwich complex. The α and β protons of the five-membered ring in **9** exhibit two distinct pseudotriplets (δ = 3.51 and 3.55 ppm), which appear in a region similar to that found for trochrocene (δ = 3.66 ppm). The highly strained character of this compound is best reflected by the signals of the cycloheptatrienyl protons, which split up into a pseudodoublet at δ = 4.68 ppm that can be assigned to the α CH groups adjacent to the bridging boron center, as well as into two multiplets for the β and γ protons (δ = 5.51 and 5.89 ppm). The large separation of the α and β protons ($\Delta\delta$ = 0.83 ppm) in combination with a significant highfield shift of the former resonance with respect to the appropriate trochrocene signal (δ = 5.45 ppm) is a characteristic feature for the presence of molecular ring strain and has previously been described for the corresponding [*n*]metalloarenophanes of chromium and manganese.[3h,25,27] Because of hindered rotation about the B−N double bond, the $SiMe_3$-groups are detected as two discrete signals at room temperature (δ = 0.37 and 0.66 ppm). The rotation barrier has been estimated by variable-temperature (VT) NMR spectroscopy and amounts to a value of ca. 67.8 KJ mol^{-1}.

As expected, the key features of the ^{1}H NMR spectrum of **9** are also present in the respective spectrum of **10**. However, the unsymmetrical substitution pattern of the nitrogen atom in **10** results in the presence of two isomers that do not interconvert at room temperature, and hence, two sets of resonance signals are observed. As a consequence, the α and β protons of the five-membered ring give rise to three multiplets (δ = 3.51, 3.56, and 3.59 ppm) with an integration ratio of 4:2:2, whereas the splitting pattern of the C_7H_6 moiety remains unmodified in comparison to **9**. In addition, both the ^{t}Bu-groups (δ = 1.53 and 1.82 ppm) and the $SiMe_3$-groups (δ = 0.42 and 0.73 ppm) are detected as two well-separated signals, and their relative intensities indicate a 1:1 mixture of the two isomers. In agreement with C_s symmetry in solution, **9** shows five signals for the ring CH carbon atoms (between δ = 74.26 and 101.89 ppm), whereas, as expected, the isomers of **10** exhibit ten

(32) (a) Hoppe, I.; Marsch, M.; Harms, K.; Boche, G.; Hoppe, D. *Angew. Chem.* **1995**, *107*, 2328−2330, *Angew. Chem. Int. Ed.* **1995**, *34*, 2158−2160. (b) Wiberg, N.; Hwang-Park, H.-S.; Mikulcik, P.; Müller, G. *J. Organomet. Chem.* **1996**, *511*, 239−253. (c) Nanjo, M.; Nanjo, E.; Mochida, K. *Eur. J. Inorg. Chem.* **2004**, 2961−2967.

(33) Zerger, R.; Rhine, W.; Stucky, G. D. *J. Am. Chem. Soc.* **1974**, *96*, 6048−6055.

(34) (a) Brown, T. L.; Seitz, L. M.; Kimura, B. Y. *J. Am. Chem. Soc.* **1968**, *90*, 3245. (b) Scovell, B. Y.; Kimura, B. Y.; Spiro, T. G. *J. Coord. Chem.* **1971**, *1*, 107.

Scheme 3. Syntheses of [1]Trochrocenophanes

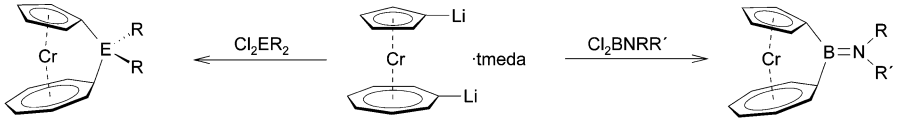

11: E = Ge, R = Me
12: E = Sn, R = Mes

8

9: R = R´ = $SiMe_3$
10: R = $SiMe_3$, R´ = ^{t}Bu

resonances (between δ = 72.53 and 100.49 ppm) in the ^{13}C NMR spectra. The ipso carbons of both compounds cannot be observed at room temperature, most probably because of the quadrupolar moment of the boron atom.[35] The ^{11}B NMR resonances (**9**, 49.9 ppm; **10**, 46.6 ppm) lie within previously reported ranges.[3d,h,15b]

To gain more detailed insight into the structural properties of **9**, the molecular structure was determined by single-crystal X-ray diffraction analysis (Figure 3). The incorporation of the small boron ansa bridge results in a substantial deviation of the aromatic rings from the coplanar arrangement observed in the unstrained precursor [Cr(η^5-C_5H_5)(η^7-C_7H_7)]. The most prominent structural feature is given by the tilting of the two aromatic ring moieties and hence, by the presence of molecular ring strain that is represented by the tilt angle α = 23.87(13)°. Because of the small covalent radius of the boron atom, this value is significantly larger than those of the corresponding [1]silatrochrocenophanes (α = 15.6° to 16.6°)[27] and suggests a notedly larger ring strain present in **9**. Yet, the values reported for the analogous boron-bridged derivatives of ferrocene [32.4(3)°][3d] and trovacene [28.2°][16b] are conspicuously higher, undoubtedly because of the longer interannular distances in these systems [cp. ferrocene (332 pm), trovacene (338 pm), and trochrocene (326 pm)]. There is also evidence that the cycloheptatrienyl systems distort in a different way to absorb strain energy than the ferrocenophanes. For instance, the trovacene derivative features a significantly lower value for *a* as expected, given the larger interannular distance with respect to ferrocene. Furthermore, the analogous bis(benzene)chromium species exhibits a larger tilt angle [26.6(3)°][15b] compared to **9**, even though the interannular distance in [Cr(η^6-C_6H_6)$_2$] is slightly diminished (322 pm). The introduction of an ansa bridge into **9** results in a significant distortion of the cycloheptatrienyl unit from planarity especially at the ipso carbon atom of the cycloheptatrienyl unit [rms deviation for Cht = 0.0553 Å and for Cp = 0.0073 Å], with the angles β between the carbocyclic ring planes and the exocyclic C−B bond of β_{Cp} = 29.9° and β_{Cht} = 43.1°. The latter appears notedly enlarged in comparison to the ferrocene derivative [33.7(2)° and 34.0(2)°].[3d] Hence, the flexibility of the seven-membered ring in **9** with respect to the cyclopentadienyl and benzene ligands of the iron and chromium congeners allows for the reduction of the molecular ring strain. Directly associated with the tilted structure of **9**, the angle δ is essentially reduced to 162.0° compared to the unstrained species **7** and **8**. The geometry around the bridging boron atom also emphasizes the highly distorted character of **9**. Even though the B−N bond length [1.399(4) Å], as well as the trigonal planar environment of the boron nucleus [ΣB = 359.9°], are in agreement with the formulation as a boron nitrogen double bond, the C_{Cp}−B−C_{Cht} angle θ = 100.52(22)° is perspicuously diminished from the ideal angle of 120° for an sp^2-hybridized boron center. Consequently, the C(arene)−B−N bond angles are widened to values of 128.47(26)° and 130.98(25)°, respectively. In addition, the highly strained geometry, particularly of the cycloheptatrienyl unit, is imposingly illustrated by the very short chromium *ipso*-C_{Cht} bond distance of 2.069(3) Å (vide supra). In contrast to these variances within the structural parameters deduced from the incorporation of an ansa bridge, the Cr−C bond lengths to the C_5H_4 ring [2.123(3)−2.219(3) Å], the chromium CH carbon bond distances to the C_7H_6 moiety [2.132(3)−2.182(3) Å], as well as the chromium centroid separation distances to the five-membered ring [1.808 Å] and the seven-membered ring [1.409 Å] are not affected.

It should be mentioned here that the presence of at least one silyl group at the nitrogen substituents is an essential prerequisite for the successful preparation of the [1]boratrochrocenophanes, most probably owing to their electronic impact.[24,28] If alkyl-substituted aminoboranes such as $Cl_2BN^iPr_2$ (vide infra), Br_2-$BNEt_2$, or Br_2BNMe_2 are employed during the synthesis, the formation of the ansa complex cannot be observed.

The introduction of the larger germanium bridge in **11** leads to the expected differences in the ^{1}H NMR spectrum compared to **9** and **10**. Even though the splitting pattern for the resonances of the aromatic ring protons has substantial similiarity to the latter, that is, two pseudotriplets are observed for the C_5H_4 ring (δ = 3.69 and 3.78 ppm), as well as one pseudodoublet (δ = 5.24 ppm) and two multiplets (δ = 5.69 and 5.83 ppm) for the C_7H_6 ring, the reduced molecular ring strain present in **11** is reflected by the diminished separation of the signals attributable to the α and β protons of the C_7H_6 moiety ($\Delta\delta$ = 0.45 ppm) in combination with the minor highfield shift of the former with respect to the corresponding resonance of trochrocene. As expected, the ^{13}C NMR spectrum displays five distinct resonance signals for the aromatic CH carbon atoms (between δ = 79.91 and 102.14 ppm) together with two more shielded signals, which can be unambiguously assigned to the *ipso*-C_5H_4 carbon atom (δ = 54.49 ppm) and to the *ipso*-C_7H_6 carbon atom (δ = 61.35 ppm). Though the molecular ring strain is supposed to be less pronounced than in **9** and **10**, the NMR spectroscopic data definitely suggest a notedly distorted molecular geometry. Given that similar NMR parameters were obtained for the appropriate [1]silatrochrocenophanes,[27] the structural properties of **11** should be more like those of the silicon species than those of the boron-bridged complexes.

To confirm the formation of a strained ansa complex, a crystal structure analysis of **11** was carried out (Figure 4). In accordance with the NMR spectroscopic data, the introduction of a monoatomic germanium bridge results in a less distorted geometry in **11** than in **9**. Whereas the Cr−C bond lengths are not affected by the larger bridge [between 2.115(3) and 2.212-(3) Å], the minor ring strain is manifested by a smaller tilt angle α = 15.07(17)°. As suspected, this value is comparable to those found in the analogous [1]silatrochrocenophanes (α = 15.6°−16.6°),[27] an effect that is related to the very similar covalent

(35) Herberhold, M.; Dörfler, U.; Wrackmeyer, B. *J. Organomet. Chem.* **1997**, *530*, 117−120.

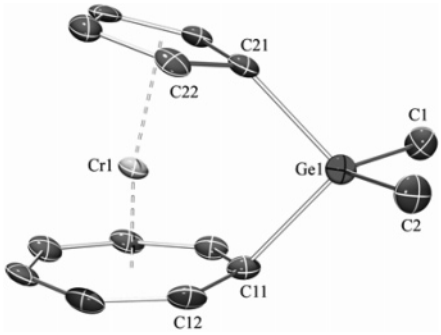

Figure 4. Molecular structure of **11**. Selected bond lengths [Å] and angles [deg]: Cr1−C11, 2.115(3); Cr1−C12, 2.140(3); Cr1−C13, 2.181(3); Cr1−C14, 2.173(3); Cr1−C15, 2.165(3); Cr1−C16, 2.174(3); Cr1−C17, 2.159(3); Cr1−C21, 2.170(3); Cr1−C22, 2.161(3); Cr1−C23, 2.216(3); Cr1−C24, 2.209(3); Cr1−C25, 2.169(3); C11−Ge1, 1.994(3); C21−Ge1, 1.971(4); Cr1−X_{Cp}, 1.820; Cr1−X_{Cht}, 1.417; C1−Ge1−*C*2, 112.55(16); C1−Ge1−C11, 114.46(15); C1−Ge1−C21, 112.37(15); *C*2−Ge1−C11, 114.17(15); *C*2−Ge1−C21, 110.94(15); C11−Ge1−C21, 90.45(13); X_{Cp}−Cr1−X_{Cht}, 168.3 (X_{Cp},, X_{Cht} = centroids of the C_5H_4 and the C_7H_6 rings, respectively).

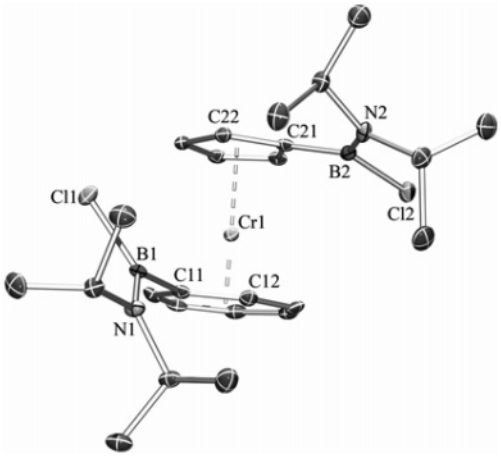

Figure 5. Molecular structure of **13**. Only one molecule of the asymmetric unit is shown for clarity. Selected bond lengths [Å] and angles [deg]: Cr1−C11, 2.198(2); Cr1−C12, 2.171(2); Cr1−C13, 2.166(2); Cr1−C14, 2.161(2); Cr1−C15, 2.167(2); Cr1−C16, 2.168(2); Cr1−C17, 2.148(2); Cr1−C21, 2.200(2); Cr1−C22, 2.185(2); Cr1−C23, 2.201(2); Cr1−C24, 2.194(2); Cr1−C25, 2.188(2); C11−B1, 1.576(4); C21−B2, 1.559(3); B1−N1, 1.391(3); B1−Cl1, 1.808(3); B2−N2, 1.398(3); B2−Cl2, 1.825(3); Cr1−X_{Cp}, 1.831; Cr1−X_{Cht}, 1.436; C11−B1−N1, 124.37(22); C11−B1−Cl1, 115.60(18); Cl1−B1−N1, 120.02(19); C21−B2−N2, 127.29(23); C21−B2−Cl2, 113.71(18); Cl2−B2−N2, 118.99(18); B1−C11−C21−B2, 89.9; X_{Cp}−Cr1−X_{Cht}, 178.0 (X_{Cp}, X_{Cht} = centroids of the C_5H_4 and the C_7H_6 rings, respectively).

radii of silicon and germanium, respectively. Again, the corresponding germanium bridged derivatives of ferrocene (19.1°)[36] and troticene (22.9°)[16c] both exhibit remarkably larger structural distortion and consequently larger tilt angles than **11** (vide supra). The distortion of the cycloheptatrienyl moiety from planarity [rms deviation for Cht = 0.0376 Å and for Cp = 0.0070 Å] is less pronounced compared to that found in **9**, whereas the angles $\beta_{Cp} = 29.8°$ and $\beta_{Cht} = 43.8°$ remain almost unchanged. Additionally, the angle $\delta = 168.3°$ is notedly enlarged with respect to that observed in **9**, whereas the silicon-bridged derivatives feature an almost identical value (δ = 167.4−168.0°), in turn. The molecular strain is also reflected by the C_{Cp}−Ge−C_{Cht} angle $\theta = 90.45(13)°$, which deviates significantly from the tetrahedral angle for a sp^3-hybridized germanium atom. The smaller angle θ results in a slight scissoring effect at germanium, with a widening of the C_{Me}−Ge−C_{Me} angle to 112.55(16)°, which has already been detected within the silicon-bridged counterparts.[27]

In contrast to the facile access to [1]trochrocenophanes containing boron, silicon, and germanium in the bridging position, the synthesis of the corresponding [1]stanna derivative caused much more difficulties. Hence, treatment of the dilithiated precursor **8**·tmeda with Cl_2SnMes_2 (Mes = 2,4,6-C_6H_2-) under various conditions did not result in the isolation of any pure material (Scheme 3). The NMR spectra obtained after workup showed a whole string of broad signals in the majority of cases, which could not be assigned to a distinct compound. This might be explained by the high lability of the Sn−C_{aryl} bond in combination with the presence of molecular ring strain. Consequently, even though the resulting species would be less strained than the boron, silicon, and germanium bridged analogues, **12** seems to be too labile for isolation. It is well documented, that the corresponding [1]stannaferrocenophanes tend to undergo thermal ROP even at room temperature depending on the substituents at the tin center.[5f] However, the desired ansa-bridged tin derivative **12** was unambiguously identified spectroscopically in the reaction mixture by means of multinuclear NMR spectroscopy. In addition, we succeeded in the isolation of a small amount (∼10 mg) of pure **12** during the workup procedure. The NMR spectroscopic data obtained from the pure sample are in accordance with a C_s-symmetric complex in solution. Thus, the aromatic ring protons of the five-membered ring exhibit two distinct pseudotriplets for the α and β positions (δ = 3.68 and 3.89 ppm), whereas the cycloheptatrienyl hydrogens are detected as two multiplets (δ = 5.60 and 5.67 ppm) with a relative ratio of 2:2:2:4. The fact, that the α protons of the C_7H_6 moiety are observed downfield shifted with respect to the respective resonance of trochrocene indicates the presence of only weak molecular ring strain in **12**; similar results were obtained with the [2]silatrochrocenophane that displays a tilt angle $\alpha = 2.60°$.[27] Additionally, the resonance signals of the *ipso*-C_5H_4 (δ = 70.36 ppm) and the *ipso*-C_7H_6 (δ = 77.43 ppm) carbon atoms in the ^{13}C NMR spectrum appear deshielded in comparison to the analogous signals of the [1]-sila and [1]germa derivatives and hence, also suggest a less distorted molecular geometry.

1,1′-Disubstituted Complexes. The syntheses of the unstrained counterparts of the [1]trochrocenophanes described above, that is, the 1,1′-disubstituted trochrocene derivatives [Cr(η^5-C_5H_4R)(η^7-C_7H_6R)] (R = B(Cl)N^{i}Pr$_2$ **13**, $SiMe_3$ **14**, $GeMe_3$ **15**, $SnMe_3$ **16**), were accomplished by treating **8**·tmeda with 2.5 equiv of the appropriate element (di)halide at −30 °C in aliphatic solvents (Scheme 4). These compounds were isolated after workup as deeply colored solids in excellent yields of 70−90%.

Compound **13** exhibits signal patterns in the ^1H NMR spectrum that emphasize the absence of molecular ring strain in this 1,1′-disubstituted metallocene. For instance, the α and β hydrogens of the five-membered ring, observed as two distinct pseudotriplets (δ = 4.34 and 4.44 ppm), appear significantly downfield shifted with respect to the corresponding resonances of both trochrocene (3.66 ppm) and the strained congeners **9**−**11**. This attribute is further supported by the resonance

(36) Foucher, D. A.; Edwards, M.; Burrow, R. A.; Lough, A. J.; Manners, I. *Organometallics* **1994**, *13*, 4959−4966.

Scheme 4. Syntheses of 1, 1′-Disubstituted Derivatives

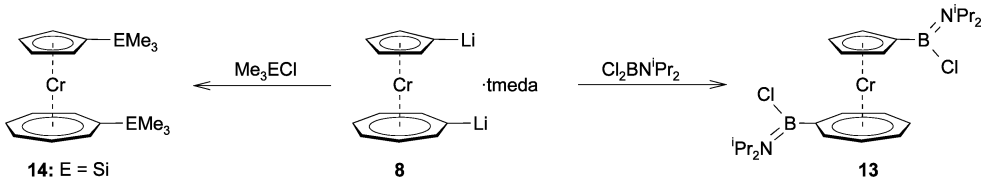

signals of the cycloheptatrienyl protons, which show one multiplet for the β and γ hydrogen atoms ($\delta = 5.79$ ppm), as well as one pseudodoublet assignable to the α protons ($\delta =$ 6.01 ppm). As described above, the protons of the seven-membered ring in α position to the substituents constitute an excellent probe for the molecular ring strain present in substituted metallocenes. Thus, the pseudodoublet is detected notedly deshielded in comparison to the appropriate trochrocene resonance ($\delta = 5.45$ ppm) and hence, suggests an only slightly distorted geometry of **13**. In contrast, the corresponding signals of the strained [*n*]trochrocenophanes are found conspicuously downfield shifted compared to the parent sandwich complex (vide supra), and the magnitude of the separation between these signals and the resonances of the β ring protons indicates even the dimension of the molecular distortion. The appearance of four distinct resonances for the ^{i}Pr-methyl groups both in the ^{1}H and the ^{13}C NMR spectrum as well as the detection of two resonance signals in the ^{11}B NMR spectrum ($\delta = 36.6$ and 39.1 ppm) definitely confirms the presence of two chemical nonequivalent boron substituents and consequently the unstrained character of **13**.

The solid-state structure of **13** was determined by X-ray diffraction (Figure 5). The asymmetric unit contains two independent molecules, whereas the structural parameters of both moieties differ only marginally. Hence, for simplicity reasons only one of the molecular structures is discussed below. The structural parameters of **13** are unremarkable with respect to the crystal structures of **7** and trochrocene,[29] save that the boryl substituents do not adopt an anti arrangement because of crystal packing effects; the angle between them amounts to 89.9°. However, both rings are virtually planar and can be considered as η^5- and η^7-coordinated, respectively. The separation distances between the chromium center and the ring centroids [Cr1−X_{Cp}, 1.831 Å; Cr1−X_{Cht}, 1.436 Å] lie within the expected range and are almost identical to those found in **7** [Cr1−X_{Cp}, 1.819 Å; Cr1−X_{Cht}, 1.439 Å] and [Cr(η^5-C_5H_5)(η^7-C_7H_7)] [Cr1−X_{Cp}, 1.830 Å; Cr1−X_{Cht}, 1.434 Å]. The absence of molecular ring strain is further reflected by the tilt angle α $= 1.81(13)°$ and the angle $\delta = 178.0°$, both indicating an almost ideal coplanar arrangement of the aromatic rings. Thus, in agreement with the NMR spectroscopic data, the geometry of the metallocene subunit exhibits only weak molecular distortion. As anticipated, the boron centers display a distorted trigonal planar environment that differs only marginally from the ideal geometry [ΣB1 = 360.0° and ΣB2 = 360.0°].

The NMR spectroscopic data of **14**−**16** can be interpreted as being caused by 1,1′-disubstituted trochrocene derivatives with time-averaged C_s-symmetry in solution. All compounds exhibit very similar signal patterns in both the ^{1}H NMR and the ^{13}C NMR spectrum that are in agreement with an unstrained molecular structure as described for **13**. Pertinent features in the ^{1}H NMR spectra include the splittings of the Cp resonances into two pseudo triplets (**14**, $\delta = 3.74$ and 3.99 ppm; **15**, $\delta =$ 3.74 and 3.98 ppm; **16**, $\delta = 3.70$ and 4.02 ppm) and of the Cht signal resonances into two multiplets (**14**, $\delta = 5.61$ and 5.68 ppm; **15**, $\delta = 5.58$ and 5.63 ppm; **16**, $\delta = 5.51$ and 5.64 ppm). Both the former and the α hydrogen atoms of the latter appear downfield shifted with respect to the resonance of trochrocene. In addition, the ^{13}C NMR spectra exhibit signals for the ipso carbon atoms of the C_5H_4 moieties (**14**, $\delta =$ 78.22 ppm; **15**, $\delta = 81.90$ ppm; **16**, $\delta = 76.61$ ppm) as well as for the ipso carbon atoms of the C_7H_6 moieties (**14**, $\delta =$ 90.31 ppm; **15**, $\delta = 94.58$ ppm; **16**, $\delta = 93.49$ ppm), which are found again significantly deshielded compared with those of the corresponding [1]trochrocenophanes. These findings are consistent with the NMR data obtained for the unstrained complex **13** and indicate the absence of molecular ring strain in these species. As expected, the ^{29}Si NMR spectrum of **14** ($\delta = -2.55$ and 6.31 ppm) and the ^{119}Sn NMR spectrum of **16** ($\delta = 0.80$ and 29.30 ppm) exhibit two distinct signal resonances for the Me_3E-substituents (E = Si, Sn) owing to chemical inequivalence of these groups.

Electronic Structure: UV−Visible Spectroscopy. To obtain information on the electronic structure of the substituted trochrocene derivatives, solution UV−vis spectra in the range of 200−800 nm were collected in thf for the species **9**, **11**, **13**−**16**, as well as for the parent compound [Cr(η^5-C_5H_5)(η^7-C_7H_7)], and the prevoiusly reported ansa trochrocenophanes **1**, **2**, and **6** (Table 1). Unsubstituted trochrocene exhibits strong UV−vis absorbances at 237 and 351 nm that can be assigned to a ligand-to-metal charge-transfer transition and transitions arising from the $1e_2$ molecular orbitals, respectively. In addition, a very weak, broad visible band is observed at 559 nm that, in analogy to ferrocene, is most probably related to excitations from the

Table 1. Experimental Determined UV−Visible Data and Calculated HOMO and LUMO Energies (eV)

	1	**2**	**6**	**9**	**11**	**12**	**13**	**14**	**15**	**16**	Tro[a]
λ_{max} (nm)	572	584	568	536	593		622	561	557	564	559
ϵ (L mol^{-1} cm^{-1})	64	60	43	151	61		76	77	68	68	29
α_{calcd} (deg)	10.0	16.2	3.3	24.8	15.1	11.9	0.7	1.6	1.3	1.3	0.0
E_{HOMO} (eV)	−4.31	−4.62	−4.59	−4.41	−4.58	4.48	−4.61	−4.62	−4.5	−4.56	−4.66
E_{LUMO} (eV)	−0.43	−0.51	−0.49	−0.57	−0.45	−0.47	−0.69	−0.50	−0.44	−0.43	−0.39
$\Delta E_{HOMO-LUMO}$ (eV)	3.89	4.11	4.09	3.84	4.13	4.02	3.92	4.11	4.14	4.13	4.27

[a] Tro = [Cr(η^5-C_5H_5)(η^7-C_7H_7)].

Table 2. Selected Calculated and Experimentally Determined (in Italics) NMR Chemical Shifts in ppm

	1[a]	**2**[b]	**6**[b]	**9**	**11**	**12**	**13**	**14**	**15**	**16**
ipso-C_5H_4	87.14	52.19	82.95	66.07	52.83	67.45	79.14	80.43	82.60	81.92
	n. o.[c]	*51.66*	*81.40*	*n. o.*[c]	*54.49*	*70.36*	*n. o.*[c]	*78.22*	*81.90*	*76.61*
ipso-C_7H_6	94.26	60.02	91.01	76.07	60.36	76,45	92.71	88.76	93.35	96.43
	n. o.[c]	*60.10*	*91.40*	*n. o.*[c]	*61.35*	*77.43*	*n. o.*[c]	*90.31*	*94.58*	*93.49*
α C_5H_4[d]	3.63	3.47	3.88	3.27	3.51	3.38	4.19	3.51	3.45	3.32
	4.05	*3.70*	*4.04*	*3.51*	*3.78*	*3.68*	*4.44*	*3.74*	*3.74*	*3.70*
α C_7H_6[d]	5.15	4.92	5.82	4.46	4.99	5.60	5.90	5.52	5.45	5.29
	5.78	*5.14*	*5.89*	*4.68*	*5.24*	*5.60*	*6.01*	*5.61*	*5.58*	*5.51*
α (deg)	10.0	16.2	3.3	24.8	15.1	11.9	0.7	1.6	1.3	1.3
	9.0(8)	*15.6(1)*	*2.6(2)*	*23.87(13)*	*15.07(17)*		*1.81(13)*			
δ (deg)	173.0	168.7	177.6	162.5	169.1	171.3	179.2	178.9	179.1	179.1
	173.1	*167.5*	*177.2*	*162.0*	*168.3*		*178.0*			

[a] Experimental values see ref 3h. [b] Experimental values see ref 27. [c] Not observed (*n. o.*). [d] Average value.

$1a_1$ molecular orbital (HOMO), which are predominantely d−d in nature and Laporte forbidden. The two highest energy bands are detected in the UV−vis spectra of all substituted complexes in an almost identical region and hence, do not reveal any differences in the electronic structure of the strained and unstrained species with respect to trochrocene. However, the corresponding lowest energy bands significantly differ from the absorbance of trochrocene depending on the molecular distortion, and the tilt angles in particular. Thus, the unstrained 1,1′-disubstituted complexes **14**−**16** containing silicon, germanium, and tin substitutents exhibit visible bands at 561, 557, and 564 nm that resemble the appropriate absorbance found in [Cr(η^5-C_5H_5)(η^7-C_7H_7)]. The increased molecular ring strain present in the [*n*]sila- (*n* = 1, **2**; *n* = 2, **6**) and [1]germatrochrocenophanes (**11**) results in a significant red-shift of these visible bands to values of 584, 568, and 593 nm, respectively. A similiar trend has been reported for the corresponding [*n*]ferrocenophanes and has been explained by a lowering of the HOMO−LUMO energy difference as the tilt angle increases.[5e] By contrast, the species bearing boron substitutents deviate notedly from this trend; in fact, they even exhibit a reverse correlation. Thus, the unstrained derivative **13** displays a very broad, conspicuously red-shifted visible band with a maximum at 622 nm, whereas the absorbance of the highly strained [1]-boratrochrocenophane **9** appears actually blue-shifted at 536 nm compared to [Cr(η^5-C_5H_5)(η^7-C_7H_7)]. A related behavior was observed in the UV−vis spectra of the corresponding [1]-boraferrocenophanes, even though the effect was much less pronounced. In this case, the smaller red-shift of these species with respect to the less strained sulfur bridged [1]ferrocenophane was attributed to the influence of subtle changes in the electronic surrounding of the bridging atom, that is, the presence of a B−N double bond.[3d] Hence, the electronic structure of substituted trochrocenes strongly depends both on the geometric arrangement as well as on the substitution pattern and the electronic environment of the ligands.

Electronic structure: DFT Calculations. To assess the differences in the electronic structure of strained and unstrained trochrocene derivatives and, hence, to obtain deeper insight into the relationship between the structural, spectroscopic, and electronic properties, DFT calculations were performed on **1**, **2**, **6**, **9**, **11**−**16** and [Cr(η^5-C_5H_5)(η^7-C_7H_7)]. The geometries of all complexes were optimized without symmetry constraints, and the structural parameters obtained showed fairly good agreement with the experimentally determined values available. Hence, the molecular structure of the species **12** and **14**−**16**, which have not yet been investigated by X-ray diffraction, can be predicted reliably, invoking the results of the calculations. A comparison of selected experimental and calculated bond lengths and angles can be found in the Supporting Information. The molecular distortion of these complexes is emphasized by the analysis of the Wiberg bond indeces (WBI) of the Cr−C bonds (see Supporting Information). In accordance with a contraction of the Cr−C bond distances to the ipso carbon atoms of the aromatic carbocylces found in the substituted trochrocene species, the corresponding WBI enlarge as the tilt angle increases. However, the alterations for the chromium ipso carbon bonds to the seven-membered ring are more significant than those to the five-membered ring. Thus, the value of the former in the highly strained derivative **9** is about 11% larger than the value found in [Cr(η^5-C_5H_5)(η^7-C_7H_7)], whereas the latter increases only about 5%. This effect is attributable to the closer arrangement of the cycloheptatrienyl moiety and the chromium center and, consequently, the larger deformation of the C_7H_6 ring with respect to the C_5H_4 ring. A similiar correlation is observed within the WBI of the Cr−C_α bonds, where the dependency on the tilt angle is much less pronounced in this case. In contrast, the calculated values for the Cr−C_β bonds exhibit a complementary trend for all investigated species and remain almost unaffected by the degree of molecular distortion for the Cr−C_γ bonds; the average WBI for the former in **9** is about 6% smaller for the Cht-ring and 4% for the Cp-ring compared to the values found in trochrocene. The quality of the DFT calculations is further supported by the calculated NMR spectroscopic chemical shifts that reflect preeminently the most prominent features associated with the molecular distortion of the substituted trochrocene derivatives (Table 2). Thus, for instance, the highfield shift of the ipso carbon atoms of both aromatic ring moieties as well as of the α C_7H_6 protons as a function of the tilt angle is very well reproduced.

To improve the understanding of the experimentally determined UV−vis spectra, we examined the molecular orbitals of trochrocene and of the substituted derivatives in more detail. In accordance with earlier experimental[37] and theoretical investigations,[38] the ground-state electronic configuration of the 18-electron sandwich complex [Cr(η^5-C_5H_5)(η^7-C_7H_7)] is $(1e_1)^4$-$(2e_1)^4(e_2)^4(a_1)^2$ (assuming infinite axes of rotation for both rings, e.g., C_{2v}). The first two virtual molecular orbitals are almost

(37) Evans, S.; Green, J. C.; Jackson, S. E.; Higgins, B. *J. Chem. Soc., Dalton Trans.* **1974**, 304−311.
(38) (a) Clack, D. W.; Warren, K. D. *J. Organomet. Chem.* 1978, *152*, C60−C62. (b) Menconi, G.; Kaltsoyannis, N. *Organometallics* **2005**, *24*, 1189−1197.

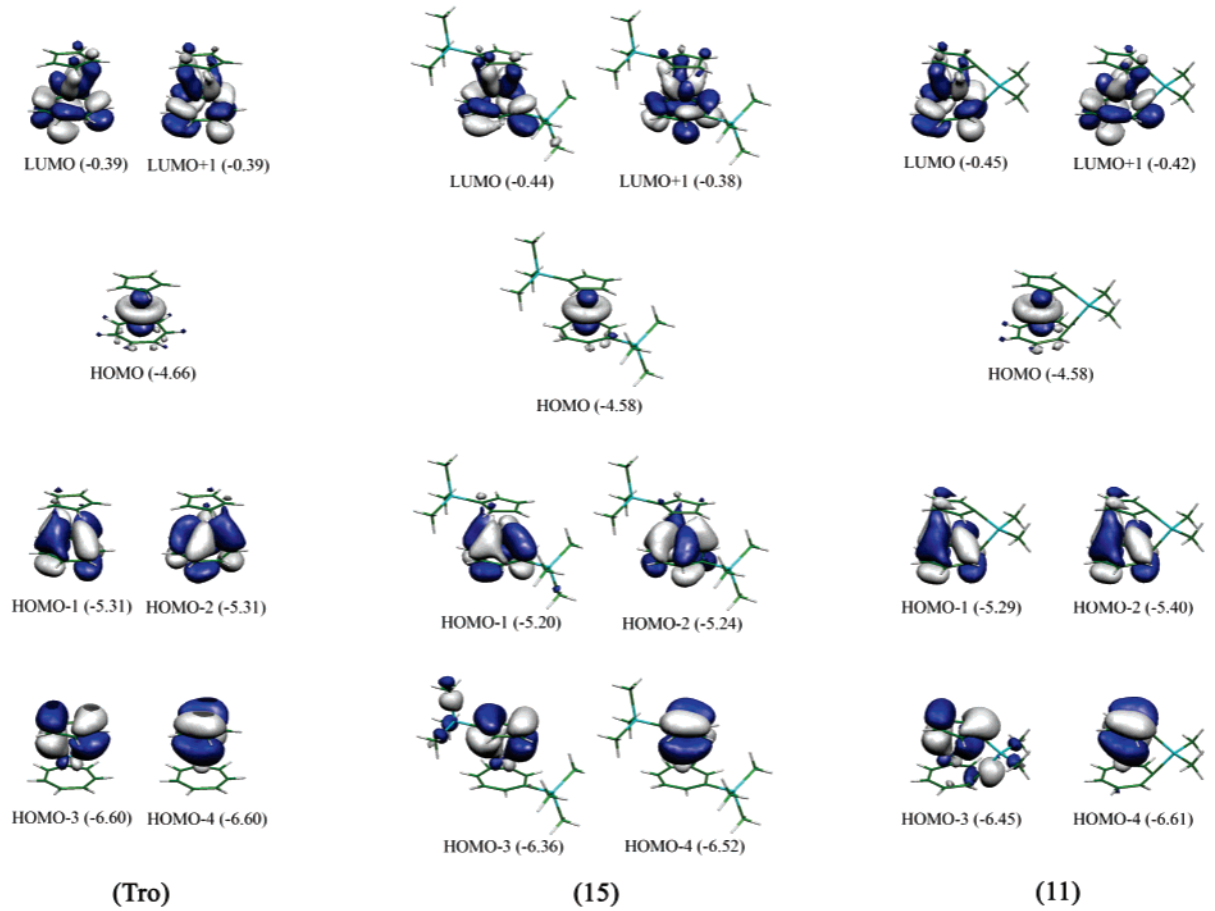

Figure 6. Contour plots and eigenvalues (eV) of selected molecular orbitals in [Cr(η^5-C_5H_5)(η^7-C_7H_7)] (left), **15** (middle), and **11** (right).

degenerate and both exhibit strong contributions from the chromium atomic orbitals (35% each) and the C_7H_7 molecular orbitals (50% each). The HOMO is essentially chromium localized (87%) with only minor contributions from the a_1 C_7H_7 MOs (10%) and hence, can be described as principally metal d in character. The next two levels are almost degenerate and arise from δ bonding between the chromium center and the cycloheptatrienyl ring. These molecular orbitals feature a significant degree of metal-ring covalency, which is reflected by a substantial contribution from both chromium (48% each) and the e_2 C_7H_7 MOs (48% each). On the contrary, the interaction of the metal center with the cyclopentadienyl ring is mainly ionic in nature. The degenerate molecular orbitals HOMO-3 and HOMO-4 are made up predominantely of the e_1 orbitals of the Cp-moiety (81% each) and thus demonstrate π bonding of the chromium and the cyclopentadienyl ring. Hence, the electronic structure of trochrocene appears to be very similiar to that found for the related titanium complex, [Ti(η^5-C_5H_5)(η^7-C_7H_7)], save that the HOMO of trochrocne refers to the LUMO of the 16-electron troticene complex.[16a] In principle, the introduction of substituents to form the 1,1′-disubstituted species **13**−**16** and the ansa-bridged complexes **1**, **2**, **6**, **9**, **11**, and **12** does not comprise the shape of the frontier orbitals described above (exceptions will be discussed later). Contour plots of these valence molecular orbitals together with their eigenvalues for trochrocene as well as representative examples of both a 1,1′-disubstituted complex (**15**) and a strained trochrocenophane (**11**) are given in Figure 6. However, the fragment contribution of the metal center, the five-membered ring and the seven-membered ring to these orbitals deviates to some extent from the values found in the unsubstituted [Cr(η^5-C_5H_5)(η^7-C_7H_7)]. In fact, a closer inspection of the contribution reveals a significant correlation of the differences as a function of the tilt angle within comparable occupied molecular orbitals. Fragments with a strong contribution loose impact on the correponding MOs as the molecular distortion increases, whereas the contribution of the other fragments become more important; however, the alterations are small and lie within a range of 1−9% (see Supporting Information). **12** seems to possess a special character that can be attributed to the presence of two additional aromatic aryl groups at the tin center. Consequently, both the sequence of the occupied molecular orbitals as well as that of the unoccupied orbitals changes substantially in comparison to the other species, and several ligand centered MOs appear within these frontier orbitals. Owing to the substitution of the two rings and the distortion of the sandwich structure, the energy position of the occupied molecular orbitals changes and the former isoenergetic MOs have given up their degeneracy. As a consequence, the HOMO−LUMO gap slightly decreases in all of the substituted species in comparison to [Cr(η^5-C_5H_5)(η^7-C_7H_7)] (Table 1). Similar observations have been reported for strained [1]ferrocenophanes. The red-shift of these compounds in the UV−vis spectra has been explained by a HOMO−LUMO transition that is lower in energy because of the decreased HOMO−LUMO-gap, which is strongly dependent on the molecular distortion.[5e] Complementary, an increase of the HOMO−LUMO gap has been offered in the explanation of the observed blue-shift in the visible spectra of strained [1]-

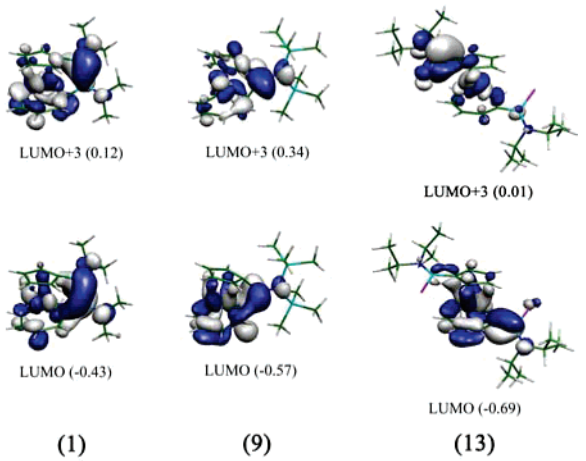

Figure 7. Contribution of the B−N π system to the LUMO (bottom) and the LUMO+3 (top) in **1**, **9**, and **13**.

silatroticenophane with respect to unsubstituted troticene; these findings are in agreement with the results obtained for strained [*n*]ferrocenophanes considering the different electronic ground-state configurations of these 16- and 18-electron species, respectively (vide supra).[17a] In our hands, this simple explanation cannot be applied; the calculated energies for the HOMO−LUMO transitions do not show any correlation to the amount of tilting present in the molecular structure of the substituted trochrocene derivatives. In fact, the magnitude of the HOMO−LUMO energy gap seems to be strongly related to the fragment contribution of the ligand to the LUMO, which is not a function of the molecular distortion (Similiar results were obtained at the HF and the MP2 level of theory).

Nevertheless, the HOMO−LUMO energy differences for the trochrocene series allow for the separation of the species into three different groups, that is, the boron containing complexes (ΔE = 3.84−3.92 eV), the compounds without boron (ΔE = 4.09−4.13 eV), and the [1]stannatrochrocenophane **12** (ΔE = 4.02 eV) (vide supra). Examination of the ten lowest lying unoccupied molecular orbitals of **1**, **9**, and **13** showed that the orbital sequence of the LUMOs in the boron containing species fundamentally changed in comparison to the other complexes. Hence, as depicted in Figure 7, the LUMO and the LUMO+3 of **1**, **9**, and **13** show significant contribution of the B−N π bond (LUMO, 30, 14, and 15%; LUMO+3, 21, 13, and 27%), whereas the fragment contribution of the substituents within the boron-free complexes is negligible in orbitals lower in energy than the LUMO+5. Thus, the complementary behavior of these compounds in the UV−vis spectra is associated to the strong electronic influence of the boron substituents and the interaction with the B−N π-system in particular. Nevertheless, the UV−vis spectoscopic data of the lowest energy band cannot be explained in detail so far, because the HOMO−LUMO transition criterion is not appropriate in the case of the substituted trochrocene derivatives. To reveal reasons for the failure of this criterion and to determine the factors that are associated with the electronic excitations in the visible area, we determined the first eight excitations of all complexes employing time-dependent density functional theory. In all of the cases, the first four calculated excitations are transitions arising from the HOMO with transition wavelengths between 527 and 641 nm, all of which can be assigned to the lowest energy band in the corresponding UV−vis spectra. The excitations together with the molecular orbitals involved in the transitions as well as the appropriate wavelengths are summarized in Table 3. According to the calculations, the absorbances observed in the UV−vis experiments consist of four distinct excitations with several orbital transitions involved in conjunction, whereas all of them feature only small transition probabilities, which is in agreement with the very weak intensities and the very broad shape of the experimentally determined visible bands. In addition, the lower energy maxima of the experiment, and consequently the correlations of λ_{max} as a function of the molecular distortion for both the boron containing and the boron-free species, are fairly well reproduced by the calculations. Hence, the lowest energy electronic excitation of substituted metallocenes observed in the UV−vis spectra is much more complicated than a simple HOMO−LUMO transition; on the contrary, a large number of transitions to a variety of LUMOs seems to be involved in these processes.

Summary and Conclusions

In this paper, the derivatization of [Cr(η^5-C_5H_5)(η^7-C_7H_7)] (trochrocene) via metalation and subsequent salt elimination reaction with element dihalides has been described in detail. To extend the chemistry of this sandwich complex, a more convenient preparative protocol has been developed that allows for the synthesis of gram quantities of [Cr(η^5-C_5H_5)(η^7-C_7H_7)]. The selectivity of its dimetalation employing ^{t}BuLi/tmeda to form the highly reactive species [Cr(η^5-C_5H_4Li)(η^7-C_7H_6Li)]·tmeda (**8**·tmeda) was confirmed by X-ray diffraction of the thf solvate [Cr(η^5-C_5H_4Li)(η^7-C_7H_6Li)]$_2$·(thf)$_8$. Structural characterization of metalated sandwich complexes is still a challenging area owing to the high reactivity of these compounds, and hence, the solution of the molecular structure of **8** contributes to the understanding of the fundamentals that determine the conformation of this class of organometallic compounds. Starting from this, novel [1]bora (**9**,**10**) and[1]germatrochrocenophanes (**11**) have been synthesized and characterized, whereas the isolation of the [1]stanna derivative **12** was hampered by its thermal lability. X-ray diffraction studies of **9** and **11** revealed the presence of strained, ring-tilted structures with tilt angles α = 23.87(13)° and 15.07(17)°, respectively. The corresponding unstrained 1,1′-disubstituted species **13**−**16** with broron, silicon, germanium, and tin connected to both aromatic rings have been prepared analogously; the molecular structure of **13** authenticated the unstrained character. According to UV−vis experiments of all compounds as well as of the previously described strained derivatives **1**, **2**, and **6**, the wave lengths of the lowest energy band was strongly depending on the molecular distortion. Within the boron-free species, these absorbances were found red-shifted with respect to trochrocene as the tilt angle increased, whereas the boron-containing derivatives showed a complementary correlation. DFT calculations revealed a strong fragment contribution of the B−N double bond to the LUMO and the LUMO+3, both involved in the excitation process. Hence, the complementary trends appeared plausible considering the strong electonic influence of the B−N π-system. Both correlations were fairly well reproduced by time dependent DFT calculations. Accordingly, the electronic excitation observed as the lowest energy band in the UV−vis spectra is a quite complicated process that is made up of four distinct excitations consisting of several transitions and arising from the respective HOMO.

Table 3. Calculated Excitations from the HOMOs and Corresponding Orbital Transitions and Transition Wave Lengths (nm)

	1	**2**	**6**	**9**	**11**	**12**	**13**	**14**	**15**	**16**	Tro[b]
first excitation	78→79 78→83 78→84 78→85 78→88	64→66 64→69 64→70	80→81 80→85 80→86 80→90 80→91	95→96 95→99	73→75 73→78 73→79 73→82	115→116 115→118 115→121 115→123 115→125 115→127 115→128	127→128 127→129 127→131 127→134 127→135 127→136	89→90 89→93 89→94 89→95	107→108 107→111 107→112 107→113	79→80 79→83 79→85	49→53 49→55
λ_1 (nm)	592.11	587.08[a]	599.3	621.42	587.45[a]	588.07[a]	641.04[a]	605.45	596.09	599.97	563.31[a]
second excitation	78→79 78→82 78→83 78→85 78→86	64→68 64→71	80→84 80→87 80→88	95→97 95→98 95→100 95→102	73→77 73→80	115→117 115→124 115→126	127→128 127→131 127→132 127→133 127→134 127→135 127→136	89→90 89→93 89→94 89→96	107→108 107→111 107→112 107→113 107→114	79→80 79→83 79→84 79→86 79→87	49→54 49→56
λ_2 (nm)	574.47[a]	580.96	570.37[a]	594.57	577.63	572.80	584.36	576.69	571.81	573.35[a]	562.02
third excitation	78→79 78→82 78→83 78→84 78→85 78→86	64→65	80→81 80→82 80→85 80→86	93→103 95→99 95→101 95→103	73→74	115→117 115→120	127→128 127→132 127→135	89→90 89→94 89→95 89→96	107→108 107→112 107→113 107→114	79→80 79→83 79→84 79→85 79→86	49→50
λ_3 (nm)	563.67	574.08	556.11	589.61	568.38	564.85	561.05	561.27[a]	555.91[a]	557.43[a]	536.13
fourth excitation	78→81	64→66 64→69 64→70 64→73	80→81 80→82	95→97 95→98 95→100 95→102 95→104 95→105	73→75 73→76 73→78 73→79 73→82	115→116 115→118 115→119 115→123 115→128	127→129 127→131	89→91 89→92	107→109 107→110	79→81 79→82	49→51
λ_4 (nm)	552.1	554.19	548.94	527.23[a]	553.16	556.58	537.93	544.32	546.27	547.74	536.11
λ_{max} (nm)	574	587	570	527	587	588	641	561	556	565	563

[a] Excitation(s) with the highest transition probability. [b] Tro = [Cr(η^5-C_5H_5)(η^7-C_7H_7)].

Experimental Section

General. All manipulations were performed under an inert atmosphere of dry argon using standard Schlenk techniques or in a glovebox. Solvents were dried according to standard procedures, freshly distilled prior to use, degassed, and stored under argon over activated molecular sieves. Deuterated solvents were distilled from potassium over a glass bridge and subjected to several freeze−pump−thaw cycles. NaCp,[39] $Cl_2BN(SiMe_3)_2$,[40] $Cl_2BN(SiMe_3)(^tBu)$,[40] $Cl_2BN^iPr_2$,[40] and Mes_2SnCl_2[41] were prepared according to known methods. Cl_2GeMe_2, Me_3SiCl, Me_3GeCl, and Me_3SnCl were obtained from Aldrich and distilled from magnesium turnings or either sublimed before use, respectively. ^{t}BuLi was purchased from Acros as 1.5 mol L^{-1} solutions in pentane. All other chemicals were obtained commercially and were used without further purification. tmeda was dried over K and distilled under argon prior to use. The NMR spectra were recorded on a Bruker DRX 300 (^{7}Li, 116.64 MHz) and on a Bruker AV 500 (^{1}H, 500.13 MHz; ^{11}B, 160.46 MHz; ^{13}C, 125.76 MHz; ^{119}Sn, 186.51 MHz) FT-NMR spectrometer. ^{1}H and ^{13}C{^{1}H} NMR spectra were referenced to external TMS via the residual protio of the solvent (^{1}H) or the solvent itself (^{13}C). ^{7}Li{^{1}H} NMR spectra were referenced to external LiCl, ^{11}B{^{1}H} NMR spectra to BF_3·OEt_2, ^{29}Si{^{1}H} NMR spectra to external TMS, and ^{119}Sn{^{1}H} NMR spectra to external Me_4Sn. Microanalyses for C, H, and N were performed on a Leco CHNS-932 elemental analyzer. UV−vis spectra were recorded on a Shimadzu UV Mini 1240 UV−vis photometer.

All SCF computations reported herein were carried out using the Gaussian 03 package running on a cluster of Linux workstations.[42] Calculations were performed using DFT methods, applying the three hybrid functional B3LYP[43−45] using 6-31G(d, p) basis functions sets for nonmetals and Stuttgart relativistic, small core ECP basis sets for metals (see Supporting Information). NMR chemical shifts calculated with the GIAO method were adjusted to TMS, Me_4Sn, or diborane(6). The latter was recalculated to the standard BF_3·Et_2O scale. The Wiberg bond indeces given in the text were obtained with the NBO 5 program.[46] Illustrations of molecular orbitals were prepared with Molekel 4.3.[47] Excitation energies were calculated using the TDDFT method included in the Gaussian 03 package.

[Cr(η^5-C_5H_5)(η^7-C_7H_7)]. Solid $CrCl_3$ (50.00 g, 316 mmol) was added to a solution of NaCp (29.00 g, 330 mmol) in thf (200 mL), and the reaction mixture was stirred at ambient temperature over a period of 24 h. Subsequently, excess Mg turnings (24.03 g, 1.00 mol) and cycloheptatriene (50 mL, 482 mmol) were added, while stirring was continued at room temperature for an additional 48 h. During this time, the color of the suspension turned to deep blue. Excess magnesium was separated by decantation; all volatiles were removed under reduced pressure, and the resulting sticky solid was carefully poured into a mixture of acetone/H_2O (1:1) under air exposure. The mixture was refluxed for 1 h, accompanied by the formation of a green solution and the precipitation of an off-white solid. The solid was filtered and treated again with refluxing acetone/H_2O. This procedure was repeated until the filtrate remained colorless. The aqueous fractions were

(39) Panda, T. K.; Gamer, M. T.; Roesky, P. W. *Organometallics* **2003**, *22*, 877−878.
(40) Haubold, W.; Kraatz, U. *Z. Anorg. Allg. Chem.* **1976**, *421*, 105−110.
(41) Brown, P.; Mahon, M. F.; Molloy, K. C. *J. Organomet. Chem.* **1992**, *435*, 265−273.
(42) Frisch, M. J.; et al. *Gaussian 03*, revision B.04; Gaussian, Inc.: Pittsburgh, PA, 2003.
(43) Becke, A. D. *J. Chem. Phys.* **1993**, *98*, 5648−5652.
(44) Vosko, S. H.; Wilk, L.; Nusair, M. *Can. J. Phys.* **1980**, *58*, 1200−1211.
(45) Lee, C.; Yang, W.; Parr, R. G. *Phys. Rev. B* **1988**, *37*, 785−789.
(46) Glendening, E. D.; Badenhoop, J. K.; Reed, A. E.; Carpenter, J. E.; Bohmann, J. A.; Morales, C. M.; Weinhold, F. *NBO5.0*; Theoretical Institute, Univeristy of Wisconsin: Madison WI, 2001.
(47) Flükiger, P.; Lüthi, H. P.; Portmann, S.; Weber J. *MOLEKEL 4.0*; Swiss Center for Scientific Computing: Manno, Switzerland, 2000.

combined and concentrated by evaporation at elevated temperature to about 300 mL yielding a bright-green solution of the trochrocene cation. The aqueous solution was layered with toluene (300 mL) and degassed with purified argon. The addition of $Na_2S_2O_4$ (50 g) and KOH (50 g) under vigorous stirring resulted in an immediate color change of the organic layer to deep blue. The toluene fraction containing the air-sensitive product was separated, and after insolubilities were separated by filtration the solvent was removed in vacuo. The residue was sublimed at 100 °C and 10^{-3} mbar to obtain 26.02 g (125 mmol, 40%) of [Cr(η^5-C_5H_5)(η^7-C_7H_7)] as a crystalline blue solid. ^{1}H NMR (500 MHz, C_6D_6, 297 K): δ = 3.66 (s, 5H, C_5H_5), 5.45 (s, 7H, C_7H_7). $^{13}C\{^1H\}$ NMR (126 MHz, C_6D_6, 297 K): δ = 75.37 (C_5H_5), 87.09 (C_7H_7). λ_{max} (ϵ) = 559 nm (29 L mol^{-1} cm^{-1}). Full characterization of trochrocene, including a crystal structure determination[29] and an accurate elemental analysis,[28c] has been reported previously.

[Cr(η^5-C_5H_4Ph)(η^7-C_7H_7)], 7. Compound **7** was isolated as a side-product formed during the synthesis of [Cr(η^5-C_5H_5)(η^7-C_7H_7)] following a slight modification of the original procedure reported by E. O. Fischer.[28] According to this, trochrocene was prepared from $CrCl_3$ (20.00 g, 126 mmol), without isolating the intermediate [Cr(η^5-C_5H_5)-(η^6-C_6H_6)]. Instead, the crude reaction was treated directly with $AlCl_3$ and cycloheptatriene to yield the trochrocene cation after hydrolysis. In addition to deep-blue crystalline trochrocene, the sublimation of the residue, obtained after the reduction of the cation with $Na_2S_2O_4$, at 100 °C and 10^{-3} mbar gave green **7** right above the heating source, which was separated mechanically from the blue main product. Pruification of crude **7** was achieved by columm chromatography (Alox III, hexane) and three recrystallization steps from hexane at −60 °C. The crystals that separated were washed with cold pentane (3 × 2 mL, −80 °C) and dried in vacuo to afford **7** as a green solid (0.56 g, 1.97 mmol, 2%). ^{1}H NMR (500 MHz, C_6D_6, 297 K): δ = 3.75 (m, 2H, C_5H_4), 4.17 (m, 2H, C_5H_4), 5.33 (s, 7H, C_7H_7), 7.35 (m, 5H, *Ph*). $^{13}C\{^1H\}$ NMR (126 MHz, C_6D_6, 297 K): δ = 73.71 (C_5H_4), 75.26 (*ipso*-C_5H_4), 76.60 (C_5H_4), 88.23 (C_7H_7), 125.68, 126.02 (*Ph*), 128.23 (*ipso*-*Ph*), 128.63 (*Ph*). Anal. Calcd (%) for $C_{18}H_{16}Cr$ (284.32): C, 76.04; H, 5.67. Found: C, 75.67; H, 5.81.

[Cr(η^5-C_5H_4Li)(η^7-C_7H_6Li)]·(thf)$_3$, 8·(thf)$_3$. Recrystallization of the dilithiated complex [Cr(η^5-C_5H_4Li)(η^7-C_7H_6Li)]·tmeda (**8**·tmeda) (0.10 g, 0.30 mmol) from a saturated thf solution (1 mL) afforded **8**·(thf)$_3$ as pale-brown crystals that were washed with cold pentane (2 × 1 mL) and dried in vacuo (0.09 g, 0.21 mmol, 70%). ^{1}H NMR (500 MHz, [D$_8$]THF, 297 K): δ = 1.75 (m, 12H, CH_2), 3.60 (m, 2H, C_5H_4), 3.85 (m, 2H, C_5H_4), 3.89 (m, 12H, OCH_2), 5.25 (m, 2H, C_7H_6), 5.33 (m, 2H, C_7H_6), 5.80 (m, 2H, C_7H_6). $^7Li\{^1H\}$ NMR (117 MHz, [D$_8$]THF, 297 K): δ = 2.40. $^{13}C\{^1H\}$ NMR (126 MHz, [D$_8$]THF, 297 K): δ = 25.32 (*C*H$_2$), 68.04 (O*C*H$_2$), 78.78, 85.73, 86.35, 91.45, 97.79 (all C_{aryl}H). Anal. Calcd (%) for $C_{24}H_{34}CrLi_2O_3$ (436.40): C, 66.05, H, 7.85. Found: C, 64.95; H, 7.01. X-ray quality crystals of the thf solvate [Cr(η^5-C_5H_4Li)(η^7-C_7H_6Li)]$_2$·(thf)$_8$ showed additional thf molecules incorporated into the crystal lattice and were obtained during the recrystallization procedure described above.

[Cr(η^5-C_5H_4)-BN(SiMe$_3$)$_2$-(η^7-C_7H_6)], 9. A slurry of **8**·tmeda (0.75 g, 2.23 mmol) in hexane (10 mL) was cooled to −78 °C and treated dropwise over a period of 2 h with a solution of $Cl_2BN(SiMe_3)_2$ (0.54 g, 2.23 mmol) in hexane (5 mL). After complete addition, the reaction mixture was stirred for an additional 5 h at −78 °C and subsequently allowed to reach ambient temperature. During this time, the color of the suspension turned from pale brown to intensive brown and a white precipitate deposited. After the solid had settled, the solution was filtered into another flask by a filter canula, and the filtrate was concentrated to about 3 mL in volume. Cooling to −60 °C afforded **9** as a dark brown solid, which was obtained analytically pure after washing with cold pentane (3 × 3 mL, −100 °C) and drying in vacuo (0.53 g, 1.41 mmol, 63%). Crystals were grown from saturated hexane solutions at −25 °C. ^{1}H NMR (500 MHz, C_6D_6, 297 K): δ = 0.37 (s, 9H, SiMe_3), 0.66 (s, 9H, SiMe_3), 3.51 (m, 2H, C_5H_4), 3.55 (m, 2H, C_5H_4), 4.68 (m, 2H, C_7H_6), 5.51 (m, 2H, C_7H_6), 5.89 (m, 2H, C_7H_6). $^{11}B\{^1H\}$ NMR (160 MHz, C_6D_6, 297 K): δ = 49.9. $^{13}C\{^1H\}$ NMR (126 MHz, C_6D_6, 297 K): δ = 5.43, 5.56 (SiMe_3), 74.26, 79.67, 86.81, 91.50, 101.89 (all C_{aryl}H). λ_{max} (ϵ) = 536 nm (151 L mol^{-1} cm^{-1}). Anal. Calcd (%) for $C_{18}H_{28}BCrNSi_2$ (377.40): C, 57.29; H, 7.48; N, 3.71. Found: C, 57.58; H, 7.20; N, 3.33.

[Cr(η^5-C_5H_4)-BN(SiMe$_3$)(^{t}Bu)-(η^7-C_7H_6)], 10. The reaction was analogously performed to that described for **9**, using **8**·tmeda (0.82 g, 2.44 mmol) in heptane (15 mL) and $Cl_2BN(SiMe_3)(^tBu)$ (0.51 g, 2.44 mmol) in heptane (5 mL). During the reaction the color of the mixture changed to deep brown and a white solid precipitated. Insolubilities were removed by filtration, and the brown filtrate was concentrated to about 4 mL in volume. Storage at −30 °C yielded a deep-brown crystalline solid (0.62 g, 1.71 mmol, 70%), which was isolated after washing with cold pentane (3 × 3 mL, −100 °C) and drying in vacuo. Compound **10** exists as a 1:1 mixture of two isomers. ^{1}H NMR (500 MHz, C_6D_6, 297 K): δ = 0.42 (s, 9H, SiMe_3), 0.73 (s, 9H, SiMe_3), 1.53 (s, 9H, CMe_3), 1.82 (s, 9H, CMe_3), 3.51 (m, 4H, C_5H_4), 3.56 (m, 2H, C_5H_4), 3.59 (m, 2H, C_5H_4), 4.72 (m, 4H, C_7H_6), 5.52 (m, 4H, C_7H_6), 5.91 (m, 2H, C_7H_6). $^{11}B\{^1H\}$ NMR (160 MHz, C_6D_6, 297 K): δ = 46.6. $^{13}C\{^1H\}$ NMR (126 MHz, C_6D_6, 297 K): δ = 6.46, 6.61 (SiMe_3), 33.50, 33.53 (CMe_3), 56.58, 57.16 (*C*Me$_3$), 72.53, 72.58, 77.89, 78.97, 85.27, 85.36, 89.97, 90.80, 100.35, 100.49 (all C_{aryl}H). Anal. Calcd (%) for $C_{19}H_{28}BCrNSi$ (361.33): C, 63.16; H, 7.81; N, 3.88. Found: C, 63.17; H, 7.67; N, 4.23.

[Cr(η^5-C_5H_4)-GeMe$_2$-(η^7-C_7H_6)], 11. A solution of Cl_2GeMe_2 (0.26 g, 1.49 mmol) in toluene (5 mL) was added over a period of 30 min to a well-stirred slurry of **8**·tmeda (0.50 g, 1.49 mmol) in toluene (20 mL) at −78 °C. The deep-blue mixture was allowed to warm to room temperature and was stirred for an additional 24 h. After the solid had settled, the solution was filtered into another flask by a filter canula and all volatiles were removed under reduced pressure. The residue was extracted over a period of 48 h with heptane. In turn, insolubilities were separated by filtration, and **11** was isolated as a dark blue solid by crystallization at −30 °C (0.28 g, 0.89 mmol, 60%). Crystals suitable for crystal structure analysis were obtained by recrystallization from thf at −80 °C. ^{1}H NMR (500 MHz, C_6D_6, 297 K): δ = 0.69 (s, 6H, CH_3), 3.69 (m, 2H, C_5H_4), 3.78 (m, 2H, C_5H_4), 5.24 (m, 2H, C_7H_6), 5.69 (m, 2H, C_7H_6), 5.83 (m, 2H, C_7H_6). $^{13}C\{^1H\}$ NMR (126 MHz, C_6D_6, 297 K): δ = 0.00 (*C*H$_3$), 54.49 (*ipso*-C_5H_4), 61.35 (*ipso*-C_7H_6), 79.91, 83.30, 88.96, 94.97, 102.14 (all C_{aryl}H). λ_{max} (ϵ) = 593 nm (61 L mol^{-1} cm^{-1}). Anal. Calcd (%) for $C_{14}H_{16}CrGe$ (308.88): C, 54.44; H, 5.22. Found: C, 54.17; H, 5.01.

Attempted synthesis of [Cr(η^5-C_5H_4)-SnMes$_2$-(η^7-C_7H_6)], 12. The synthesis of **12** was attempted under various conditions. For instance, a suspension of **8**·tmeda (0.50 g, 1.49 mmol) in hexane (10 mL) was treated dropwise with a solution of Cl_2SnMes_2 (0.64 g, 1.49 mmol) in thf (20 mL) at −78 °C. Upon the slurry being warmed to ambient temperature the color changed to blue-brown and an off-white solid deposited. After the slurry was stirred for a further 12 h, all volatiles were removed in vacuo, the residue was extracted with Et_2O, and insolubilities were separated by filtration. The dark blue filtrate was concentrated to about 7 mL in volume and stored at −30 °C in the freezer. After several days, a small crop of a brownish, crystalline material separated, which was subsequently isolated by decantation and drying under high vacuum. This material turned out to be pure **12** (0.01 g, 17.75 μmol, 1%). However, the isolation of additional **12** failed in all cases, and the materials isolated instead could not be identified. ^{1}H NMR (500 MHz, C_6D_6, 297 K): δ = 2.12 (s, 6H, CH_3), 2.86 (s, 12H, CH_3), 3.68 (m, 2H, C_5H_4), 3.89 (m, 2H, C_5H_4), 5.60 (m, 2H, C_7H_6), 5.67 (m, 4H, C_7H_6), 6.91 (s, 4H, $C_6H_2Me_3$). $^{13}C\{^1H\}$ NMR (126 MHz, C_6D_6, 297 K): δ = 21.10, 25.34 (*C*H$_3$), 70.36 (*ipso*-C_5H_4), 77.43 (*ipso*-C_7H_6), 82.91, 86.77, 95.02, 98.72 (all C_{aryl}H), 129.22, 137.32, 139.45, 145.57 ($C_6H_2Me_3$). $^{29}Sn\{^1H\}$ NMR (187 MHz, C_6D_6, 297 K): δ = −61.92.

[Cr{η^5-$C_5H_4B(Cl)N^iPr_2$}{η^7-$C_7H_6B(Cl)N^iPr_2$}], 13. A suspension of **8**·tmeda (0.60 g, 1.78 mmol) in hexane (10 mL) was added rapidly to a well-stirred solution of $Cl_2BN^iPr_2$ (0.81 g, 4.46 mmol, 2.5 equiv) in hexane (10 mL) at room temperature. Upon stirring for 18 h the color of the slurry changed from brown to deep green. After the solid had settled, the solution was filtered into another flask by a filter canula, and the filtrate was concentrated to about 10 mL in volume to yield greenish crystals of **13** (0.62 g, 1.25 mmol, 70%) upon cooling to −35 °C, which were subsequently washed with cold pentane (3 × 2 mL, −100 °C) and dried in vacuo. X-ray quality crystals were grown from saturated heptane solutions at −25 °C. ^{1}H NMR (500 MHz, C_6D_6, 297 K): δ = 0.80 (d, ^3J(H, H) = 6.70 Hz, 6H, *Me*), 0.96 (d, ^3J(H, H) = 6.70 Hz, 6H, *Me*), 1.59 (d, ^3J(H, H) = 6.63 Hz, 6H, *Me*), 1.60 (d, ^3J(H, H) = 6.63 Hz, 6H, *Me*), 3.24 (m, 2H, C*H*Me$_2$), 4.05 (m, 1H, C*H*Me$_2$), 4.27 (m, 1H, C*H*Me$_2$), 4.34 (m, 2H, C_5H_4), 4.44 (m, 2H, C_5H_4), 5.79 (m, 4H, C_7H_6), 6.01 (m, 2H, C_7H_6). ^{11}B{^{1}H} NMR (160 MHz, C_6D_6, 297 K): δ = 36.6, 39.1. ^{13}C{^{1}H} NMR (126 MHz, C_6D_6, 297 K): δ = 21.48, 21.74, 23.70, 24.32 (*Me*), 46.53, 46.67, 50.89, 52.06 (*C*HMe$_2$), 81.26, 84.05, 88.06, 88.90, 91.51 (all C_{aryl}H). λ_{max} (ϵ) = 622 nm (76 L mol^{-1} cm^{-1}). Anal. Calcd (%) for $C_{24}H_{38}B_2Cl_2CrN_2$ (499.10): C, 57.76; H, 7.67; N, 5.61. Found: C, 58.05; H, 7.44; N, 5.83.

[Cr(η^5-$C_5H_4SiMe_3$)(η^7-$C_7H_6SiMe_3$)], 14. In a procedure analogous to the preparation of **13**, employing **8**·tmeda (0.50 g, 1.49 mmol) in pentane (10 mL) and Me_3SiCl (0.40 g, 3.72 mmol, 2.5 equiv) in pentane (10 mL) afforded **14** (0.41 g, 1.16 mmol, 78%) as a dark-blue solid after recrystallization and drying in vacuo. ^{1}H NMR (500 MHz, C_6D_6, 297 K): δ = 0.26 (s, 9H, Si*Me*$_3$), 0.48 (s, 9H, Si*Me*$_3$), 3.74 (m, 2H, C_5H_4), 3.99 (m, 2H, C_5H_4), 5.61 (m, 4H, C_7H_6), 5.68 (m, 2H, C_7H_6). ^{13}C{^{1}H} NMR (126 MHz, C_6D_6, 297 K): δ = 0.10, 0.36 (Si*Me*$_3$), 78.22 (*ipso*-C_5H_4), 78.38, 79.69, 87.49, 88.46, 90.14 (all C_{aryl}H), 90.31 (*ipso*-C_7H_6). ^{29}Si{^{1}H} NMR (99.4 MHz, C_6D_6, 297 K): δ = −2.55, 6.31. λ_{max} (ϵ) = 561 nm (77 L mol^{-1} cm^{-1}). Anal. Calcd (%) for $C_{18}H_{28}CrSi_2$ (352.58): C, 61.32; H, 8.00. Found: C, 60.97; H, 7.88.

[Cr(η^5-$C_5H_4GeMe_3$)(η^7-$C_7H_6GeMe_3$)], 15. In a procedure analogous to the preparation of **13**, employing **8**·tmeda (0.40 g, 1.19 mmol) in pentane (10 mL) and Me_3GeCl (0.46 g, 2.97 mmol, 2.5 eq.) in pentane (10 mL) afforded **15** (0.45 g, 1.02 mmol, 86%) as a dark-blue solid after recrystallization and drying in vacuo. ^{1}H NMR (500 MHz, C_6D_6, 297 K): δ = 0.39 (s, 9H, Ge*Me*$_3$), 0.57 (s, 9H, Ge*Me*$_3$), 3.74 (m, 2H, C_5H_4), 3.98 (m, 2H, C_5H_4), 5.58 (m, 4H, C_7H_6), 5.63 (m, 2H, C_7H_6). ^{13}C{^{1}H} NMR (126 MHz, C_6D_6, 297 K): δ = 0.03, 0.20 (Ge*Me*$_3$), 78.28, 79.76 (C_{aryl}H), 81.90 (*ipso*-C_5H_4), 87.79, 88.69, 90.31 (C_{aryl}H), 94.58 (*ipso*-C_7H_6). λ_{max} (ϵ) = 557 nm (68 L mol^{-1} cm^{-1}). Anal. Calcd (%) for $C_{18}H_{28}CrGe_2$ (441.63): C, 48.95; H, 6.39. Found: C, 49.14; H, 6.40.

[Cr(η^5-$C_5H_4SnMe_3$)(η^7-$C_7H_6SnMe_3$)], 16. In a procedure analogous to the preparation of **13**, employing **8**·tmeda (0.35 g, 1.04 mmol) in hexane (10 mL) and Me_3SnCl (0.52 g, 2.60 mmol, 2.5 eq.) in hexane (15 mL) afforded **16** (0.50 g, 0.94 mmol, 90%) as an analytically pure, dark-blue solid. ^{1}H NMR (500 MHz, C_6D_6, 297 K): δ = 0.32 (s, $^2J_{HCSn}$ = 52.49 and 54.85 Hz, 9H, Sn*Me*$_3$), 0.45 (s, $^2J_{HCSn}$ = 50.60 and 52.88 Hz, 9H, Sn*Me*$_3$), 3.70 (m, 2H, C_5H_4), 4.02 (m, 2H, C_5H_4), 5.51 (m, 2H, C_7H_6), 5.64 (m, 4H, C_7H_6). ^{13}C{^{1}H} NMR (126 MHz, C_6D_6, 297 K): δ = −8.04, −7.57 (Sn*Me*$_3$), 76.61 (*ipso*-C_5H_4), 78.77, 81.71, 87.80, 89.49, 92.93 (all C_{aryl}H), 93.49 (*ipso*-C_7H_6). ^{119}Sn{^{1}H} NMR (187 MHz, C_6D_6, 297 K): δ = 0.81, 29.30. λ_{max} (ϵ) = 564 nm (68 L mol^{-1} cm^{-1}). Anal. Calcd (%) for $C_{18}H_{28}CrSi_2$ (533.83): C, 40.50; H, 5.29. Found: C, 40.63; H, 5.44.

Crystal Structure Determinations. The crystal data of **7**, **8**·(thf)$_4$, **9**, **11**, and **13** were collected on a Bruker Apex diffractometer with a CCD area detector and graphite monochromated Mo Kα radiation The structures were solved using direct methods, refined with the Shelx software package (Sheldrick, G. *Shelx*; University of Göttingen: Göttingen, Germany, 1997) and expanded using Fourier techniques. All non-hydrogen atoms were refined anisotropically. Hydrogen atoms were assigned idealized positions and were included in structure factor calculations. The crystals of **7** were nonmerohedrical twins arising from 180° rotation about the reciprocal axis 001. Integration was performed for two domains and an absorption correction was done with the twinabs program. Refinement against HKLF5 formated F^2 gave BASF = 0.14.

Crystal Data for 7. $C_{18}H_{16}Cr$, M_r = 284.31, green plate, 0.18 × 0.11 × 0.03 Å^3, monoclinic space group $P2_1$, a = 10.7402(8) Å, b = 7.7821(6) Å, c = 15.8286(11) Å, β = 97.715(4)°, V = 1311.00(17) Å,^{3} Z = 4, ρ_{calcd} = 1.440 g·cm^{-3}, μ = 0.853 mm^{-1}, F(000) = 592, T = 100(2) K, R_1 = 0.0336, wR^2 = 0.0879, 3943 independent reflections [$2\theta \le 52.14°$], and 344 parameters.

Crystal Data for 8$_2$·(thf)$_8$. $C_{56}H_{84}Cr_2Li_4O_8$, M_r = 1016.99, brown block, 0.20 × 0.13 × 0.06 Å^3, monoclinic space group $P2_1/n$, a = 10.2885(3) Å, b = 28.3264(9) Å, c = 18.4643(6) Å, β = 94.224(2)°, V = 5366.5(3) Å^3, Z = 4, ρ_{calcd} = 1.259 g·cm^{-3}, μ = 0.457 mm^{-1}, F(000) = 2176, T = 100(2) K, R_1 = 0.0675, wR^2 = 0.1837, 11106 independent reflections [$2\theta \le 53.08°$], and 782 parameters.

Crystal Data for 9. $C_{18}H_{28}BCrNSi_2$, M_r = 377.40, brown plate, 0.18×.011 × 0.02, triclinic space group $P\bar{1}$, a = 6.4925(3) Å, b = 9.8498(4) Å, c = 15.5959(7) Å, α = 104.538(2)°, β = 99.734(2)°, γ = 93.165(2)°, V = 946.52(7) Å^3, Z = 2, ρ_{calcd} = 1.324 g·cm^{-3}, μ = 0.729 mm^{-1}, F(000) = 400, T = 293(2) K, R_1 = 0.0580, wR^2 = 0.1099, 3691 independent reflections [$2\theta \le 52.2°$] and 208 parameters.

Crystal Data for 11. $C_{14}H_{16}CrGe$, M_r = 308.86, green needle, 0.24 × 0.06 × 0.03 Å^3, monoclinic space group $P2_1/n$, a = 10.9050(6) Å, b = 7.8237(5) Å, c = 14.4488(8) Å, β = 92.614(3)°, V = 1231.45(12) Å,^{3} Z = 4, ρ_{calcd} = 1.666 g·cm^{-3}, μ = 3.291 mm^{-1}, F(000) = 624, T = 100(2) K, R_1 = 0.0402, wR^2 = 0.0818, 2433 independent reflections [$2\theta \le 52.16°$], and 146 parameters.

Crystal Data for 13. $C_{24}H_{38}B_2Cl_2CrN_2$, M_r = 499.08, green plate, 0.12 × 0.08 × 0.03 Å^3, monoclinic space group $P2_1$, a = 10.8739(2) Å, b = 14.2066(3) Å, c = 16.5281(4) Å, β = 99.7530(10)°, V = 2516.38(9) Å,^{3} Z = 4, ρ_{calcd} = 1.317 g·cm^{-3}, μ = 0.682 mm^{-1}, F(000) = 1056, T = 100(2) K, R_1 = 0.0302, wR^2 = 0.0709, 9914 independent reflections [$2\theta \le 52.04°$], and 559 parameters.

Crystallographic data are also deposited with Cambridge Crystallographic Data Centre. Copies of the data [**7**−**9**, **11**, **13**: CCDC 642176−642180] can be obtained free of charge via www.ccdc.cam.ac.uk/data_request/cif, by e-mailing data_request@ccdc.cam.ac.uk, or by contacting the Cambridge Crystallographic Data Centre, 12, Union Road, Cambridge CB 1EZ, U.K. Fax +44 1223 336033.

Acknowledgment. This work was supported by the DFG. T.K. thanks the FCI for a stipend. We are grateful to the BASF AG for a generous donation of chemicals.

Supporting Information Available: Complete ref 42; crystallographic data in CIF format; tables of selected calculated and experimental determined geometrical and NMR spectroscopic parameters for all compounds; plots of the calculated WBIs of the Cr−C bonds as a function of the tilt angle α; dependency of the calculated fragment contributions of the chromium center, the C_5H_4-ring, and the C_7H_6-ring to selected frontier molecular orbitals as a function of the tilt angle α. This material is available free of charge via the Internet at http://pubs.acs.org.

JA0724947